Charles University in Prague
Faculty of Mathematics and Physics

MASTER THESIS

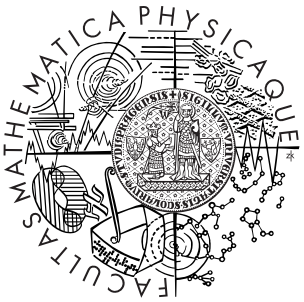

Petr Šimánek

Interaction of compressible fluid with bodies

Department of Numerical Mathematics

Supervisor: Prof. RNDr. Miloslav Feistauer, DrSc., dr. h. c.
Study branch: Numerical and Computational Mathematics

2010

I would like to thank to all who supported me in my master study and during the work on this thesis. I would like to express my gratitude to my supervisor Prof. RNDr. Miloslav Feistauer, DrSc., dr. h. c. for his many advices and comments and his nice and motivating approach during all my study years. I would like to thank RNDr. Václav Kučera, Ph.D. for his many practical remarks, valuable information and computer code. Last but not least, I am in debt to my family and my close friends, whose support and patience made this work possible.

I confirm that I prepared the master thesis by my own, and that I listed all used sources of information in the bibliography. I agree with lending the master thesis.

In Prague, April 19, 2010 Petr Šimánek

Contents

List of Figures

Název práce: Interakce stlačitelného proudění s obtékanými tělesy
Autor: Petr Šimánek
Katedra: Katedra numerické matematiky
Vedoucí diplomové práce: Prof. RNDr. Miloslav Feistauer, DrSc., dr. h. c.
e-mail vedoucího: feist@karlin.mff.cuni.cz

Abstrakt: V předložené práci studujeme interakci vazkého i nevazkého proudění stlačitelné tekutiny s leteckým profilem. Jsou zde popsány a odvozeny Eulerovy a Navier-Stokesovy rovnice. Je uvedna prostorová a časová diskretizace těchto rovnic v časové závislé oblasti s pomocí nespojité Galerkinovy metody konečných prvků. Pro řešení problému v časově proměnných oblastech používáme ALE metodu. Jsou odvozeny rovnice popisující pohyb leteckého profilu se dvěma stupni volnosti. V závěru jsou uvedeny výsledky pro předepsaný pohyb profilu i interakce vazkého i nevazkého proudění. Prezentovány jsou výsledky subsonického i transonického proudění.

Klíčová slova: Interakce proudění a struktur, Stlačitelné proudění, ALE metoda, Nespojitá Galerkinova metoda konečných prvků, Subsonické proudění, Transonické proudění

Title: Interaction of compressible fluid with bodies
Author: Petr Šimánek
Department: Department of Numerical Mathematics
Supervisor: Prof. RNDr. Miloslav Feistauer, DrSc., dr. h. c.
Supervisor's e-mail address: feist@karlin.mff.cuni.cz

Abstract: In the present work we study interaction of compressible viscous and inviscid flow with airfoil. We describe Euler equations and compressible Navier-Stokes equations. The space and time discretization of these equations in time-dependent domains is made with the aid of the discontinuous Galerkin finite element method (DGFEM). To study the flow in the time-dependent domains the Arbitrary Lagrangian-Eulerian (ALE) method is used. The equations describing motion of airfoil with two degrees of freedom are derived. We present and compare results of the flow with prescribed airfoil motion and of fluid-structure interaction for both viscous and inviscid flow. We present subsonic and transonic results.

Keywords: Fluid-structure interaction, Compressible flow, ALE method, Discontinuous Galerkin finite element method, Subsonic flow, Transonic flow

Introduction

The fluid-structure interaction plays a fundamental role in many engineering branches, e.g. aircraft development, mechanical engineering (turbomachinery - vibration of blades), civil engineering (bridge flutter), nuclear engineering, biotechnology etc. The interaction between fluid flow and moving structures is studied in aeroelasticity or hydroelasticity. To perform the aeroelastic computation means to combine the CFD computation with the structural dynamics and elasticity. Good understanding of aeroelastic processes and good ability to predict them is very important, because the aeroelastic effects can lead to undesired or even dangerous results (noise generation, material wear, building or bridge collapse, aircraft crash etc.).

This thesis is concerned with numerical solution of the air-airfoil interaction. The study of airfoil aeroelastic stability is important for aeroelastic design of aircrafts. With new advanced materials and new construction methods the designers and constructors aim at lighter and more flexible airfoils. This reduction of stiffness makes the airfoil susceptible to the aeroelastic instability. Therefore, we need to be able to accurately predict the occurring interactions.

We deal with 2D compressible viscous and inviscid flow in a time-dependent domain. It is necessary to consider compressible flow, because the operational Mach numbers of usual public aircrafts are too high to use the incompressible flow model (e.g. the "cruising speed" of Airbus A340 corresponds to Mach number 0.82).

The flow is described by equations representing conservation laws - the Euler and Navier-Stokes equations, the continuity equation and the energy equation together with some boundary conditions and an initial condition. We solve this system of partial differential equations by the discontinuous Galerkin finite element method (DGFEM). This numerical method is suitable for high-order space discretization and for the use on unstructed grids. It can be also efficiently parallelized, which is necessary for "real life" problems. Since we assume the time-dependent domain, we have to use suitable technique working on moving meshes. The Arbitrary Lagrangian-Eulerian (ALE) method is used.

This thesis is structured as follows. In Chapter 1 the Euler and Navier-Stokes equations as well as the energy and the continuity equations are derived. We also present some thermodynamical relations which are necessary in the following.

In Chapter 2 we present DGFE discretization of the Euler equations, treat the boundary conditions and outline the shock capturing technique, which is necessary to avoid the Gibbs phenomenon in case of transonic flow. We also present the DGFE discretization of the Euler equations in time-dependent domains and details of the ALE method. The DGFE discretization of the Navier-Stokes equations in time-dependent domains is performed in Chapter 3. In Chapter 4 we derive the equations describing the motion of an airfoil with two degrees of freedom. In Chapter 5 we describe some of the techniques used in our test calculations. The last chapter summarises results obtained for prescribed airfoil motion and fluid-structure interaction.

Chapter 1

Equations governing compressible flow

This chapter describes some basic flow properties, conservation laws and their mathematical form. We pay special attention to Navier-Stokes equations governing compressible flow.

1.1 Description of the flow

Let $(0,T) \subset I\!R$ be a time interval and $\Omega_t \subset I\!R^3$ be a space occupied by a fluid at time $t \in (0,T)$. We assume the so-called *fundamental hypothesis*

exactly one fluid particle passes through each point $x \in \Omega_t$ at time t.

Fluid motion can be described in two ways:
I) The Lagrangian description considers motion of each fluid particle. Trajectory of one particle can be described by

$$x = \varphi(X,t).$$

X is the reference determining the particle. Components X_1, X_2, X_3 of the reference X are called *Lagrangian coordinates*. The velocity of the particle with reference X is defined as

$$\hat{\boldsymbol{v}}(X,t) = \frac{\partial \varphi}{\partial t}(X,t). \tag{1.1}$$

The acceleration of the particle is defined as

$$\hat{\mathbf{a}}(X,t) = \frac{\partial^2 \varphi}{\partial t^2}(X,t). \tag{1.2}$$

II) The Eulerian description is used to determine the velocity of the particle

passing through the point x at time t. Following (1.1), we write the velocity $\boldsymbol{v}(x,t)$ at the point x and time t as

$$\boldsymbol{v}(x,t) = \hat{\boldsymbol{v}}(X,t) = \frac{\partial \varphi}{\partial t}(X,t) \quad \text{where} \quad x = \varphi(X,t). \tag{1.3}$$

Similarly, following (1.2), the acceleration of the particle passing through x at time t is expressed as

$$\mathbf{a}(x,t) = \frac{\partial \boldsymbol{v}}{\partial t}(x,t) + \sum_{i=1}^{3} v_i(x_i,t)\frac{\partial \boldsymbol{v}}{\partial x_i}(x,t). \tag{1.4}$$

We can also write

$$\mathbf{a} = \frac{\partial \boldsymbol{v}}{\partial t} + (\boldsymbol{v} \cdot grad)\boldsymbol{v} = \frac{\partial \boldsymbol{v}}{\partial t} + (\boldsymbol{v} \cdot \nabla)\boldsymbol{v}. \tag{1.5}$$

We can now introduce notation

$$\frac{\mathrm{D}}{\mathrm{D}t} = \frac{\partial}{\partial t} + (\boldsymbol{v} \cdot grad) = \frac{\partial \boldsymbol{v}}{\partial t} + (\boldsymbol{v} \cdot \nabla). \tag{1.6}$$

We call this symbol the *material derivative* with respect to time. The material derivative consists of the local derivative ($\frac{\partial}{\partial t}$) and the convective derivative ($\boldsymbol{v} \cdot \mathrm{grad}$). Now we can see that the acceleration $\mathbf{a}$ is the material derivative of the velocity.

Transition from Eulerian to Lagrangian description is equivalent to the determination of the trajectory of a particle when we know the velocity field. The trajectory of the particle passing through the point $X \subset \Omega_{t_0}$ at time $t \in (0,T)$ is the solution of the initial value problem

$$\frac{d\boldsymbol{x}}{dt} = \boldsymbol{v}(\boldsymbol{x},t), \quad \boldsymbol{x}(t_0) = X. \tag{1.7}$$

We can formulate theorem describing the uniqueness and the existence of solution of (1.7), proven in [6].

1.2 The transport theorem

In this section we introduce the *transport theorem*. Consider some physical quantity and a function $\boldsymbol{F} = \boldsymbol{F}(\boldsymbol{x},t)$ representing this quantity. Let $\mathcal{V}(t) \subset \Omega_t$ be a bounded domain occupied by fluid at time t. The total amount $\mathcal{F}(t)$ of the quantity represented by $\boldsymbol{F}$ that is in the volume $\mathcal{V}(t)$ at time t is defined by

$$\mathcal{F}(t) = \int_{\mathcal{V}(t)} \boldsymbol{F}(\boldsymbol{x},t)d\boldsymbol{x}. \tag{1.8}$$

We also need to define the rate of change of the quantity $\mathcal{F}$:

$$\frac{d\mathcal{F}(t)}{dt} = \frac{d}{dt}\int_{\mathcal{V}(t)} \boldsymbol{F}(\boldsymbol{x},t)d\boldsymbol{x}. \tag{1.9}$$

Suppose that $\boldsymbol{F} \in \mathcal{C}^1(\mathcal{M})$ and $\boldsymbol{v} \in [\mathcal{C}^1(\mathcal{M})]^3$. Let $\varphi = \varphi(X, t_0; t)$ be the solution of (1.7) (we know, that this solution exists and is unique). This mapping defines how the domain $\mathcal{V}(t)$ changes with time. If t_0 is an arbitrary time instant and $\mathcal{V}(t) \subset \Omega_{t_0}$, then

$$\mathcal{V}(t) = \{\varphi(X, t_0; t);\ X \in \mathcal{V}(t_0)\}. \tag{1.10}$$

We further denote the Jacobian $\mathcal{J}(X,t)$ of the mapping

$$X \in \mathcal{V}(t_0) \longrightarrow \varphi(\mathbf{X}, t_0; t) \in \mathcal{V}(t) \tag{1.11}$$

as

$$\mathcal{J}(X,t) = \det\frac{D\varphi(X,t_0;t)}{DX} = \det\begin{pmatrix} \frac{\partial\varphi_1}{X_1}, & \frac{\partial\varphi_1}{X_2}, & \frac{\partial\varphi_1}{X_3} \\ \frac{\partial\varphi_2}{X_1}, & \frac{\partial\varphi_2}{X_2}, & \frac{\partial\varphi_2}{X_3} \\ \frac{\partial\varphi_3}{X_1}, & \frac{\partial\varphi_3}{X_2}, & \frac{\partial\varphi_3}{X_3} \end{pmatrix}.$$

We state auxiliary lemma before we proceed to the transport theorem.

Lemma 1.1 *Let $t_0 \in (0,T)$, $\mathcal{V}(t_0)$ be a bounded domain with $\overline{\mathcal{V}(t_0)} \subset \Omega_{t_0}$. Then there exists an interval (t_1,t_2) (where $t_0 \in (t_1,t_2)$) such that:*

1. *The mapping (1.11) with $t \in (t_1,t_2)$ has continuous first order derivatives with respect to t, X_1, X_2, X_3 and continuous second derivatives $\partial^2\varphi/\partial t\partial X_i$, $i = 1,2,3$.*

2. *The mapping (1.11) is a continuously differentiable one-to-one mapping, that maps $\mathcal{V}(t_0)$ onto $\mathcal{V}(t)$. The mapping has the Jacobian which is continuous and bounded and satisfies the condition*

$$\mathcal{J}(X,t) > 0 \quad \forall X \in \mathcal{V}(t_0), \quad \forall t \in (t_1,t_2).$$

3. *The inclusion*

$$\left\{(\boldsymbol{x},t);\ t \in [t_1,t_2],\ \boldsymbol{x} \in \overline{\mathcal{V}(t)}\right\} \subset \mathcal{M}$$

holds true and so the mapping $\boldsymbol{v}$ (from (1.7)) has continuous and bounded first derivatives on $\{(\boldsymbol{x},t);\ t \in (t_1,t_2),\ \boldsymbol{x} \in \mathcal{V}(t)\}$.

4. $\boldsymbol{v}(\varphi(X,t_0;t),t) = \frac{\partial\varphi}{\partial t}(X,t_0;t) \quad \forall X \in \mathcal{V}(t_0), \forall t \in (t_1,t_2)$.

Proof can be found in [6].

Theorem 1.2 *Let conditions 1) - 4) from Lemma 1.1 be satisfied and let the function* $\boldsymbol{F} = \boldsymbol{F}(\boldsymbol{x}, t)$ *have continuous and bounded first order derivatives on the set* $\{(\boldsymbol{x}, t); t \in (t_1, t_2), \boldsymbol{x} \in \mathcal{V}(t)\}$. *Then for each* $t \in (t_1, t_2)$ *there exists the finite derivative*

$$\begin{aligned}
&\frac{d\mathcal{F}_{ht}}{dt}(t) = \frac{d}{dt}\int_{\mathcal{V}(t)} \boldsymbol{F}(\boldsymbol{x}, t)d\boldsymbol{x} \\
&= \int_{\mathcal{V}(t)} \left[\frac{\partial \boldsymbol{F}}{\partial t}(\boldsymbol{x}, t) + \boldsymbol{v}(\boldsymbol{x}, t) \cdot grad\, \boldsymbol{F}(\boldsymbol{x}, t) + \boldsymbol{F}(\boldsymbol{x}, t) div \boldsymbol{v}(\boldsymbol{x}, t)\right] d\boldsymbol{x} \\
&= \int_{\mathcal{V}(t)} \left[\frac{\partial \boldsymbol{F}}{\partial t}(\boldsymbol{x}, t) + div(\boldsymbol{F}\boldsymbol{v})(\boldsymbol{x}, t)\right] d\boldsymbol{x}.
\end{aligned}$$

Proof can be found in [6].

In the next sections we shall introduce the mathematical formulation of some fundamental physical laws, called *conservation laws*. We can assemble couples of conservation laws and their mathematical formulations: the law of conservation of mass - the continuity equation, the law of conservation of momentum - the equations of motion and the law of conservation of energy - the energy equation.

1.3 The continuity equation

The *density of fluid* is a function

$$\rho : \mathcal{M} = \{(\boldsymbol{x}, t); t \in (0, T), \boldsymbol{x} \in \Omega_t\} \to (0, +\infty). \tag{1.12}$$

In virtue of this definition we can compute the mass $m(\mathcal{V}; t)$ of the fluid contained in any subdomain $\mathcal{V} \subset \Omega_t$ as

$$m(\mathcal{V}; t) = \int_{\mathcal{V}} \rho(\boldsymbol{x}, t)d\boldsymbol{x}. \tag{1.13}$$

Suppose $\rho \in C^1(\mathcal{M})$ and $\boldsymbol{v} \in [C^1(\mathcal{M})]^3$. Let us consider an arbitrary time point $t_0 \in (0, T)$ and a moving system of fluid particles which fills a bounded domain $\mathcal{V} \subset \overline{\mathcal{V}} \subset \Omega_{t_0}$ at the time t_0. $\mathcal{V}$ is called *control volume*. Further we denote the domain filled by the considered system of fluid particles at the time $t \in (t_1, t_2)$ by $\mathcal{V}(t)$, where $t_0 \in (t_1, t_2)$ and this time interval has properties from Lemma 1.1. This means that $\mathcal{V}(t_0) = \mathcal{V}$ and conditions 1) - 4) from Lemma 1.1 are satisfied.

Then we can formulate the *conservation of mass* in the following way:
The mass of the piece of fluid represented by the domain $\mathcal{V}(t)$ *does not depend on time* t.

This means that

$$\frac{dm(\mathcal{V}(t); t)}{dt} = 0, \qquad t \in (t_1, t_2). \tag{1.14}$$

In virtue of (1.13),

$$m(\mathcal{V}(t);t) = \int_{\mathcal{V}(t)} \rho(\boldsymbol{x},t)d\boldsymbol{x}. \tag{1.15}$$

As said before, the presumptions of the transport theorem 1.2 are satisfied for the function $\boldsymbol{F} = \rho$ and by using this theorem, from (1.14) and (1.15) we get

$$\frac{d}{dt}\int_{\mathcal{V}(t)} \rho(\boldsymbol{x},t)d\boldsymbol{x} = \int_{\mathcal{V}(t)} \left[\frac{\partial \rho}{\partial t}(\boldsymbol{x},t) + div(\rho \boldsymbol{v})(\boldsymbol{x},t)\right] d\boldsymbol{x} = 0, \quad t \in (t_1,t_2).$$

Now we can substitute $t := t_0$ and because it holds $\mathcal{V}(t_0) = \mathcal{V}$ we obtain

$$\int_{\mathcal{V}} \left[\frac{\partial \rho}{\partial t}(\boldsymbol{x},t_0) + div(\rho \boldsymbol{v})(\boldsymbol{x},t_0)\right] d\boldsymbol{x} = 0 \tag{1.16}$$

for an arbitrary $t_0 \in (0,T)$ and an arbitrary control volume $\mathcal{V} \subset \Omega_{t_0}$.

For the next step we need the following lemma. We will use it to derive the differential form of the mass conservation law.

Lemma 1.3 *Let $\Omega \subset I\!R^3$ be an open set, $f \in C(\Omega)$. Then*

$$f \equiv 0 \text{ in } \Omega \quad \Leftrightarrow \quad \int_{\mathcal{V}} f dx = 0 \text{ for any open and bounded set } \mathcal{V} \subset \overline{\mathcal{V}} \subset \Omega.$$

Proof: The proof is elementary and we will verify both implications.

'$\Rightarrow$' If $f \equiv 0$ then $\int_{\mathcal{V}} f dx = 0 \ \ \forall\, \mathcal{V} \subset \Omega$.

'$\Leftarrow$' Let us suppose the contradiction:
Let $\int_{\mathcal{V}} f dx = 0$ for each $\mathcal{V} \subset \overline{\mathcal{V}} \subset \Omega$ and there exists $x_0 \in \Omega$ such that $f(x_0) > 0$. We know that f is continuous. Then there exists a neighborhood $U(x_0)$ such that $f(x) > 0$ for each $x \in U(x_0)$. It means that $\int_{U(x_0)} f dx > 0$, which is the contradiction with the assumption.

□

Now, using the continuity of the integrand in (1.16), Lemma 1.3 and writing t instead of t_0, we obtain the relationship

$$\frac{\partial \rho}{\partial t}(\boldsymbol{x},t) + div(\rho(\boldsymbol{x},t)\boldsymbol{v}(\boldsymbol{x},t)) = 0, \qquad t \in (0,T),\ \boldsymbol{x} \in \Omega_t. \tag{1.17}$$

This equation represents the differential form of the law of conservation of mass and is called the *continuity equation*.

1.4 The equations of motion

Now we would like to derive basic equations describing the fluid motion. They will be drawn from the *law of conservation of momentum* which says:
The rate of change of the total momentum of a piece of fluid formed by the same particles at each time and occupying the domain $\mathcal{V}(t)$ at time t is equal to the force acting on $\mathcal{V}(t)$.

Let us suppose $\rho \in C^1(\mathcal{M}), \boldsymbol{v} \in [C^1(\mathcal{M})]^3$. The total momentum of fluid particles contained in $\mathcal{V}(t)$ is given by

$$\boldsymbol{\mathcal{H}}(\mathcal{V}(t)) = \int_{\mathcal{V}(t)} \rho(\boldsymbol{x},t)\boldsymbol{v}(\boldsymbol{x},t)d\boldsymbol{x}.$$

Further we can denote by $\boldsymbol{\mathcal{F}}(\mathcal{V}(t))$ the force acting on the volume $\mathcal{V}(t)$ and then the law of conservation of momentum reads

$$\frac{d\boldsymbol{\mathcal{H}}(\mathcal{V}(t))}{dt} = \boldsymbol{\mathcal{F}}(\mathcal{V}(t)), \qquad t \in (t_1,t_2).$$

The transport theorem can be used in this step and we obtain

$$\int_{\mathcal{V}(t)} \left[\frac{\partial}{\partial t}(\rho(\boldsymbol{x},t)v_i(\boldsymbol{x},t)) + div(\rho(\boldsymbol{x},t)v_i(\boldsymbol{x},t)\boldsymbol{v}(\boldsymbol{x},t))\right]d\boldsymbol{x} = \mathcal{F}_i(\mathcal{V}(t)),$$
$$i = 1,2,3, t \in (t_1,t_2).$$

Now, taking into account that $t_0 \in (0,T)$ is an arbitrary time instant and $\mathcal{V}(t_0) = \mathcal{V} \subset \overline{\mathcal{V}} \subset \Omega_{t_0}$, where $\mathcal{V}$ is an arbitrary control volume, we can write t instead of t_0 in the law of conservation of momentum and we get

$$\int_{\mathcal{V}} \left[\frac{\partial}{\partial t}(\rho(\boldsymbol{x},t)v_i(\boldsymbol{x},t)) + div(\rho(\boldsymbol{x},t)v_i(\boldsymbol{x},t)\boldsymbol{v}(\boldsymbol{x},t))\right]d\boldsymbol{x} = \mathcal{F}_i(\mathcal{V};t) \qquad (1.18)$$

for $i = 1,2,3$, an arbitrary time $t \in (0,T)$ and an arbitrary control volume $\mathcal{V} \subset \Omega_t$. The vector $\boldsymbol{\mathcal{F}}(\mathcal{V};t)$ with components $\mathcal{F}_i(\mathcal{V};t)$ denotes the force acting on the volume $\mathcal{V}$ at the time t.

Our aim is to derive differential equation from (1.18). For that we need to characterize the vector $\boldsymbol{\mathcal{F}}(\mathcal{V};t)$. We can distinguish two types of forces acting in fluids and we introduce them now.

1. The *volume force* (also called outer or body force) $\boldsymbol{\mathcal{F}}_v(\mathcal{V};t)$ acting at the time t on the particles contained in a control volume $\mathcal{V} \subset \overline{\mathcal{V}} \subset \Omega_t$ is expressed by its density related to the unit of mass $\boldsymbol{f} \in [C(\mathcal{M})]^3$:

   $$\boldsymbol{\mathcal{F}}_v(\mathcal{V};t) = \int_{\mathcal{V}} \rho(\boldsymbol{x},t)\boldsymbol{f}(\boldsymbol{x},t)d\boldsymbol{x}. \qquad (1.19)$$

   Volume forces are for example gravitation and electromagnetic or electrostatic forces.

2. The *surface force* (or inner force because it is caused by inner interactions inside the fluid) $\boldsymbol{\mathcal{F}}_s(\mathcal{V};t)$ represents the activity of the fluid contained outside the control volume $\mathcal{V}$ at the time t on this volume. It is expressed by means of the *stress vector* $\mathbb{T}(\boldsymbol{x},t,\boldsymbol{n})$ characterizing the density of the surface force, where $\boldsymbol{n}$ is the unit outer normal to $\mathcal{V}$. We assume that $\mathbb{T} \in [C(\mathcal{M}\times S_1)]^3$, where S_1 is the surface of the unit sphere with center at the origin. Then we have

$$\boldsymbol{\mathcal{F}}_s(\mathcal{V};t) = \int_{\partial\mathcal{V}} \mathbb{T}(\boldsymbol{x},t,\boldsymbol{n}(\boldsymbol{x}))dS. \tag{1.20}$$

Now the stress vector $\mathbb{T}(\boldsymbol{x},t,\boldsymbol{n})$ can be expressed with the aim of some of its values for certain normals. Let us choose the normals parallel to the coordinate axes and set

$$\tau_{ji} = T_i(\boldsymbol{x},t,\boldsymbol{e}_j), \qquad i,j=1,2,3,$$

where $\boldsymbol{e}_j$ are unit vectors with directions of coordinate axes. The quantities $\tau_{ji} = \tau_{ji}(\boldsymbol{x},t), i,j=1,2,3$ are called the components of the *stress tensor* (for more informations about stress tensor see [6])

$$\mathcal{T} = \begin{pmatrix} \tau_{11}, & \tau_{12}, & \tau_{13} \\ \tau_{21}, & \tau_{22}, & \tau_{23} \\ \tau_{31}, & \tau_{32}, & \tau_{33} \end{pmatrix}.$$

Then we can write

$$T_i(\boldsymbol{x},t,\boldsymbol{n}) = \sum_{j=1}^{3} n_j \tau_{ji}(\boldsymbol{x},t), \qquad i=1,2,3. \tag{1.21}$$

Let us assume that $\rho, v_i, \tau_{ij} \in C^1(\mathcal{M})$ and $f_i \in C(\mathcal{M}), i,j=1,2,3$. Substituting $\mathcal{F}_i(\mathcal{V};t)$ in (1.18) we obtain

$$\int_{\mathcal{V}} \left[\frac{\partial}{\partial t}(\rho(\boldsymbol{x},t)v_i(\boldsymbol{x},t)) + div(\rho(\boldsymbol{x},t)v_i(\boldsymbol{x},t)\boldsymbol{v}(\boldsymbol{x},t))\right] d\boldsymbol{x} =$$

$$= \int_{\mathcal{V}} \rho(\boldsymbol{x},t) f_i(\boldsymbol{x},t) d\boldsymbol{x} + \int_{\partial\mathcal{V}} \sum_{j=1}^{3} \tau_{ji}(\boldsymbol{x},t) n_j(\boldsymbol{x}) dS, \qquad i=1,2,3,$$

for each $t \in (0,T)$ and for an arbitrary control volume $\mathcal{V} \subset \Omega_t$.

Now using Green's theorem we get the *equations of motion of a general fluid in differential conservative form*

$$\frac{\partial}{\partial t}(\rho v_i) + div(\rho v_i \boldsymbol{v}) = \rho f_i + \sum_{j=1}^{3} \frac{\partial \tau_{ji}}{\partial x_j}, \qquad i=1,2,3,$$

which can be written also as

$$\frac{\partial}{\partial t}(\rho\boldsymbol{v}) + div(\rho\boldsymbol{v}\otimes\boldsymbol{v}) = \rho\boldsymbol{f} + div\,\mathcal{T}. \tag{1.22}$$

1.5 The Navier-Stokes equations

The relations between the stress tensor and other quantities describing the fluid flow, particularly the velocity and its derivatives, are represented by the so-called *rheological equations* of the fluid.

The form of the stress tensor is presented. The proof of this statement can be found in [6]. Under some conditions (Stoke's postulates, see [6]) the stress tensor has the form

$$\mathcal{T} = (-p + \lambda\, div\, \boldsymbol{v})\mathbb{I} + 2\mu\mathbb{D}(\boldsymbol{v}), \tag{1.23}$$

where λ, μ are constants or scalar functions of thermodynamical quantities.

If the stress tensor depends linearly on the velocity deformation tensor as in (1.23), we call the fluid *Newtonian*. This is the common case of fluids. Gases are always Newtonian.

Let us assume that $\rho \in C^1(\mathcal{M})$ and $\frac{\partial \boldsymbol{v}}{\partial t}$ and $\frac{\partial^2 \boldsymbol{v}}{\partial x_i \partial x_j} \in C(\mathcal{M}), i, j = 1, 2, 3,$ and substitute relation (1.23) into the general equations of motion (1.22). We get the so-called *Navier-Stokes equations*

$$\frac{\partial(\rho \boldsymbol{v})}{\partial t} + div(\rho \boldsymbol{v} \otimes \boldsymbol{v}) = \rho \boldsymbol{f} - grad\, p + grad(\lambda\ div\, \boldsymbol{v}) + div(2\mu\mathbb{D}(\boldsymbol{v})), \tag{1.24}$$

where μ and λ are called the first and the second viscosity coefficients. Sometimes we call μ dynamical viscosity too.

In the kinetic theory of gases the conditions

$$\mu \geq 0, \qquad 3\lambda + 2\mu \geq 0 \tag{1.25}$$

are derived. There holds the relation $3\lambda + 2\mu = 0$ for monoatomic gases. This condition is also usually used as simplification for more complicated gases. In this papers we shall assume that both μ and λ are constants.

Now we derive another forms of Navier-Stokes equations which we are going to use later.

Let us assume that ρ and $\boldsymbol{v}$ are sufficiently regular and satisfy the continuity equation (1.17), and that the viscosity coefficients μ and λ are constants.

An important quantity in viscous flow is the so-called *Reynolds number*, defined as

$$Re = \frac{U^* L^* \rho^*}{\mu^*}, \tag{1.26}$$

where U^* is the characteristic velocity, L^* is is the characteristic length, ρ^* is the characteristic density and μ^* is is the characteristic viscosity of the given configuration.

1.6 The equation of energy

In this section energy equation will be derived. This equation represents law of conservation of energy formulated as: *The rate of change of the total energy of the fluid particles occupying the domain $\mathcal{V}(t)$ at time t is equal to the sum of the power of the volume force acting on the volume $\mathcal{V}(t)$ and the power of the surface force acting on the surface $\mathcal{V}(t)$, and of the amount of heat transmitted to $\mathcal{V}(t)$*. Let us denote by $\mathcal{E}(\mathcal{V}(t))$ the total energy of the fluid particles contained in the domain $\mathcal{V}(t)$ and by $\mathcal{Q}(\mathcal{V}(t))$ the amount of heat transmitted to $\mathcal{V}(t)$ at time t. Taking into account the character of outer and inner forces acting on the domain $\mathcal{V}(t)$, determined by the density $\boldsymbol{f}$ of the volume force and the stress vector $\mathbb{T}$, we get the representation of the law of conservation of energy

$$\begin{aligned}\frac{d}{dt}\mathcal{E}(\mathcal{V}(t)) &= \int_{\mathcal{V}(t)} \rho(x,t)\boldsymbol{f}(x,t)\cdot\boldsymbol{v}(x,t)dx \\ &+ \int_{\partial\mathcal{V}(t)} \mathbb{T}(x,t,\boldsymbol{n}(x))\cdot\boldsymbol{v}(x,t)dS + \mathcal{Q}(\mathcal{V}(t)).\end{aligned} \tag{1.27}$$

We further introduce the relations

$$\begin{aligned}&\mathcal{E}(\mathcal{V}(t)) = \int_{\mathcal{V}(t)} E(x,t)dx, \\ &E = \rho(e + \frac{|\boldsymbol{v}|^2}{2}), \\ &\mathcal{Q}(\mathcal{V}(t)) = \int_{\mathcal{V}(t)} \rho(x,t)q(x,t)dx - \int_{\partial\mathcal{V}(t)} \boldsymbol{q}(x,t)\cdot\boldsymbol{n}(x)dS.\end{aligned} \tag{1.28}$$

Here we denote E as total energy, e as specific internal energy, $\frac{|\boldsymbol{v}|^2}{2}$ as density of the kinetic energy, q as density of heat sources (related to unit of mass) and $\boldsymbol{q}$ as heat flux. We can write

$$\int_{\partial\mathcal{V}(t)} \boldsymbol{q}(x,t)\cdot\boldsymbol{n}(x)dS = -\int_{\partial\mathcal{V}(t)} k(x,t)\frac{\partial\theta(x,t)}{\partial n}dS, \tag{1.29}$$

with help of *Fourier's law*

$$\boldsymbol{q} = -k\,\mathrm{grad}\theta, \tag{1.30}$$

where k is the heat conductivity coefficient and θ is absolute temperature. From *second law of thermodynamics* it can be proven, that $k \geq 0$. Coefficient k depends on absolute temperature but we suppose that k is constant. Taking

into account (1.21) and (1.28) we can write (1.27)

$$\frac{d}{dt}\int_{\mathcal{V}(t)} E(x,t)dx = \int_{\mathcal{V}(t)} \rho(x,t)\boldsymbol{f}(x,t)\cdot\boldsymbol{v}(x,t)dx + \int_{\partial\mathcal{V}(t)} \sum_{j=1}^{3} \tau_{ji}(x,t)n_j(x)v_i(x,t)dS \qquad (1.31)$$
$$+ \int_{\mathcal{V}(t)} \rho(x,t)q(x,t)dx - \int_{\partial\mathcal{V}(t)} \boldsymbol{q}(x,t)\cdot\boldsymbol{n}(x)dS.$$

We assume that $\rho,\ v_i,\ \tau_{ij},\ q_i \in \mathcal{C}^1(\mathcal{M})$ and $f_i,\ q \in \mathcal{C}(\mathcal{M}),\ (i,j=1,2,3)$. As a result of transport and Green theorem and Lemma 1.5, *energy equation* in differential conservative form can be derived as

$$\frac{\partial E}{\partial t} + div(E\boldsymbol{v}) = \rho\boldsymbol{f}\cdot\boldsymbol{v} + div\,\mathcal{T}\boldsymbol{v} + \rho q - div\,\boldsymbol{q}. \qquad (1.32)$$

1.7 Thermodynamical relations

We need to add some additional equations to make conservative law system complete. We call the absolute temperature θ, the density ρ and the pressure p *state variables*. All these variables are positive functions. The gas is characterized by the equation of state

$$p = p(\rho,\theta) \quad \text{and} \quad e = e(\rho,\theta).$$

It is then possible to express p and θ as a functions of e and ρ

$$p = p(e,\rho) \quad \text{and} \quad \theta = \theta(e,\rho).$$

We often consider *perfect gas*. Then the state variables satisfy equation of state in the form

$$p = R\theta\rho, \qquad (1.33)$$

where $R > 0$ is the *gas constant*, which can be expressed in the form

$$R = c_p - c_v, \qquad (1.34)$$

c_p is *specific heat at constant pressure* and c_v is *specific heat at constant volume*. We know from experiments that $c_p > c_v$ and so $R > 0$. We call quantity

$$\gamma = \frac{c_p}{c_v} > 1 \qquad (1.35)$$

Poisson adiabatic constant. The internal energy of a perfect gas is given by $e = c_v\theta$.

Chapter 2

Discontinuous Galerkin finite element method

In this chapter we shall be concerned with the discontinuous Galerkin finite element method (DGFEM). We apply the method on equations describing compressible inviscid flow - the Euler equations.

2.1 DGFEM discretization of Euler equations

Let us consider the unsteady flow of an inviscid gas in a domain $\Omega \subset \mathbb{R}^2$. It is governed by the continuity equation, the Euler equations of motion and the energy equation, to which we add thermodynamical relations from previous section. This system is simply called the Euler equations. We assume adiabatic flow and so we neglect heat transfer. Moreover, we neglect the outer volume force, because the gas is light. We shall be concerned with the flow of a perfect gas.

Further, we define disjoint boundary parts $\Gamma_I,\ \Gamma_O,\ \Gamma_W$, the *inlet*, *outlet* and *impermeable wall* respectively, $\Gamma_I \cup \Gamma_O \cup \Gamma_W = \partial\Omega$. Next we set $\Gamma_{IO} = \Gamma_I \cup \Gamma_O$. The system of the Euler equations describing 2D inviscid compressible flow can be written in form

$$\frac{\partial \boldsymbol{w}}{\partial t} + \sum_{s=1}^{2} \frac{\partial \boldsymbol{f}_s(\boldsymbol{w})}{\partial x_s} = 0 \quad \text{in } Q_T, \tag{2.1}$$

where $Q_T = \Omega \times (0,T),\ \Omega \subset \mathbb{R}^2,\ T > 0$, $\boldsymbol{w}(x,t)$ is the state vector and $\boldsymbol{f}_1, \boldsymbol{f}_2$ are the inviscid fluxes

$$\begin{aligned} \boldsymbol{w} =& (\rho, \rho v_1, \rho v_2, E)^T \in \mathbb{R}^4, \\ \boldsymbol{f}_i =& (f_{i1}(\boldsymbol{w}), \ldots, f_{i4}(\boldsymbol{w})) \\ =& (\rho v_i, \rho v_1 v_i + \delta_{1i} p, \rho v_2 v_i + \delta_{2i} p, (E+p) v_i)^T. \end{aligned} \tag{2.2}$$

We use the relation

$$p = (\gamma - 1)(e - \rho|\boldsymbol{v}|^2/2). \tag{2.3}$$

We prescribe initial condition

$$\boldsymbol{w}(x, 0) = \boldsymbol{w}_0(x) \quad x \in \Omega. \tag{2.4}$$

Boundary conditions will be discussed in Section (2.1.3). In the following, we need a property of the fluxes called *homogeneity*:

$$\boldsymbol{f}_s(\alpha \boldsymbol{w}) = \alpha \boldsymbol{f}_s(\boldsymbol{w}), \quad \alpha \in I\!R,\ \alpha \neq 0,\ s = 1, 2. \tag{2.5}$$

This implies relation

$$\boldsymbol{f}_s(\boldsymbol{w}) = \mathbb{A}_s(\boldsymbol{w})\boldsymbol{w}, \quad \text{where } \mathbb{A}_s(\boldsymbol{w}) = \frac{D\boldsymbol{f}_s(\boldsymbol{w})}{D\boldsymbol{w}},\ s = 1, 2. \tag{2.6}$$

We define the *speed of sound*

$$a = \sqrt{\gamma p/\rho} \tag{2.7}$$

and the *Mach number*

$$M = \frac{|\boldsymbol{v}|}{a}. \tag{2.8}$$

The speed of sound is the velocity of the propagation of perturbations in density and pressure. In other words, the speed of sound is the highest speed that "information" travels in a compressible fluid. Further we define the *entropy*:

$$S = c_v \ln \frac{p/p_0}{(\rho\rho_0)^\gamma}, \tag{2.9}$$

where p_0 and ρ_0 are a reference pressure and density. Assume $\boldsymbol{n} = (n_1, n_2)^T \in I\!R^2$ with $|\,\boldsymbol{n}| = 1$. Let

$$\mathbb{P}(\boldsymbol{w}, \boldsymbol{n}) := \sum_{s=1}^{2} \mathbb{A}_s(\boldsymbol{w}) n_s, \tag{2.10}$$

$$\mathcal{P}(\boldsymbol{w}, \boldsymbol{n}) := \sum_{s=1}^{2} f_s(\boldsymbol{w}) n_s. \tag{2.11}$$

We can now write following lemma proved in [6].

Lemma 2.1 *(Diagonal hyperbolicity) Let $\boldsymbol{n} = (n_1, n_2)^T \in I\!R^2$ with $|\boldsymbol{n}| = 1$. Then the matrix $\mathbb{P}(\boldsymbol{w}, \boldsymbol{n})$ is diagonalizable with real eigenvalues, i.e. there exists a matrix $\mathbb{T} \in I\!R^{4,4}$ and $\lambda_1, \ldots, \lambda_4 \in I\!R$ such that*

$$\mathbb{P}(\boldsymbol{w}, \boldsymbol{n}) = \mathbb{T}\mathbb{D}\mathbb{T}^{-1}, \quad \mathbb{D} = \mathrm{diag}(\lambda_1, \ldots, \lambda_4). \tag{2.12}$$

2.1.1 Space discretization

Let Ω_h be a polygonal approximation of Ω. By T_h we denote a partition of Ω_h consisting of elements $K_i \in T_h$, $i \in I$, e.g. triangles or quadrilaterals and $I \subset \mathbb{Z}^+$ is suitable set of indexes. By Γ_{ij} we denote a common edge between neighboring elements K_i and K_j. We set $s(i) = \{j \in I,\ K_j \text{ is a neighboring element of } K_i\}$. The boundary $\partial\Omega_h$ of polygonal approximation of Ω is formed by finite number of faces of elements K_i adjacent to $\partial\Omega_h$. By S_j we denote all these boundary faces, where $j \in I^b \subset \mathbb{Z}^-$. Now we set $\gamma(i) = j \in I^b,\ S_j$ is face of $K_i \in T_h$ and $\gamma_{ij} = S_j$ for $K_i \in T_h$ such that $S_j \subset \partial K_i,\ j \in I^b$. We set $\gamma(i) = \emptyset$ for K_i not containing any boundary face S_j. Then $s(i) \cap \gamma(i) = \emptyset$ for all $i \in I$. If we write $S(i) = s(i) \cup \gamma(i)$, we have

$$\partial K_i = \bigcup_{j \in S(i)} \Gamma_{ij}, \quad \partial K_i \cap \partial\Omega_h = \bigcup_{j \in \gamma(i)} \Gamma_{ij}. \tag{2.13}$$

The symbol $\boldsymbol{n}_{ij} = ((n_{ij})_1, (n_{ij})_2)$ denotes outer unit normal to ∂K_{ij} on the face Γ_{ij}.

We will search the approximate solution at each time instant t as an element of the finite-dimensional space

$$\mathbf{S}_h = \mathbf{S}^{r,-1}(\Omega_h, T_h) = \{\varphi_h;\ \varphi_h|_K \in P^r(K)\ \forall K \in T_h\}^4, \tag{2.14}$$

where $r > 0, r \in \mathbb{N}$ and P^r denotes the space of polynomials of degree $\leq r$ on K. Functions $\varphi \in \mathbf{S}_h$ are generally discontinuous on interfaces Γ_{ij}. By $\varphi|_{\Gamma_{ij}}$ and $\varphi|_{\Gamma_{ji}}$ we denote the values of φ on Γ_{ij} considered from the interior and exterior of K_i, respectively. We define the *average* and the *jump* of a function φ on Γ_{ij} as

$$\langle\varphi\rangle_{ij} = \frac{1}{2}(\varphi|_{\Gamma_{ij}} + \varphi|_{\Gamma_{ji}}), \quad [\varphi]_{ij} = \varphi|_{\Gamma_{ij}} - \varphi|_{\Gamma_{ji}}. \tag{2.15}$$

We will now derive the discrete problem. We assume that the exact solution $\boldsymbol{w}$ is sufficiently regular (e.g. continuously differentiable in $\overline{\Omega} \times [0, T]$). We multiply the Euler equations (2.1) by an arbitrary test function $\varphi \in \mathbf{S}_h$ and integrate over all elements $K_i \in T_h$. Applying Green's theorem and summing up over all $i \in I$, we obtain

$$\begin{aligned} \frac{d}{dt} \sum_{K_i \in T_h} \int_{K_i} \boldsymbol{w}(t) \cdot \varphi d\boldsymbol{x} = \sum_{K_i \in T_h} \int_{K_i} \sum_{s=1}^{2} \boldsymbol{f}_s(\boldsymbol{w}(t)) \cdot \frac{\partial \varphi}{\partial x_s} d\boldsymbol{x} \\ - \sum_{K_i \in T_h} \sum_{j \in S(i)} \int_{\Gamma_{ij}} \sum_{s=1}^{2} \boldsymbol{f}_s(\boldsymbol{w}(t))(n_{ij})_s \cdot \varphi dS. \end{aligned} \tag{2.16}$$

We approximate the fluxes through the faces Γ_{ij} using numerical flux $\boldsymbol{H} = \boldsymbol{H}(\boldsymbol{u}, \boldsymbol{w}, \boldsymbol{n})$ in the form

$$\int_{\Gamma_{ij}} \sum_{s=1}^{2} \boldsymbol{f}_s(\boldsymbol{w})(n_{ij})_s \cdot \varphi dS \approx \int_{\Gamma_{ij}} \boldsymbol{H}(\boldsymbol{w}_h|_{\Gamma_{ij}}, \boldsymbol{w}_h|_{\Gamma_{ji}}, \boldsymbol{n}_{ij}) \cdot \varphi dS. \tag{2.17}$$

We introduce the forms

$$(\boldsymbol{w}_h, \varphi_h)_h = \int_{\Omega_h} \boldsymbol{w}_h \cdot \varphi_h d\boldsymbol{x}, \tag{2.18}$$

$$\begin{aligned} \widetilde{b}_h(\boldsymbol{w}_h, \varphi_h) = &- \sum_{K_i \in T_h} \int_{K_i} \sum_{s=1}^{2} \boldsymbol{f}_s(\boldsymbol{w}_h(t)) \cdot \frac{\partial \varphi_h}{\partial x_s} d\boldsymbol{x} \\ &+ \sum_{K_i \in T_h} \sum_{j \in S(i)} \int_{\Gamma_{ij}} \boldsymbol{H}(\boldsymbol{w}_h|_{\Gamma_{ij}}, \boldsymbol{w}_h|_{\Gamma_{ji}}, \boldsymbol{n}_{ij}) \cdot \varphi_h dS. \end{aligned} \tag{2.19}$$

Now we can define the *approximate solution* of (2.1) as a function $\boldsymbol{w}_h$ satisfying the conditions

$$\boldsymbol{w}_h \in C^1([0,T]; \mathbf{S}_h), \tag{2.20}$$

$$\frac{d}{dt}(\boldsymbol{w}_h, \varphi_h)_h + \widetilde{b}_h(\boldsymbol{w}_h, \varphi_h) = 0, \quad \forall \varphi_h \in \mathbf{S}_h, \ \forall t \in (0,T), \tag{2.21}$$

$$\boldsymbol{w}_h(0) = \Pi_h \boldsymbol{w}^0, \tag{2.22}$$

where $\Pi_h \boldsymbol{w}^0$ is the L^2-projection of $\boldsymbol{w}^0$ from the initial condition

$$\boldsymbol{w}(\boldsymbol{x}, 0) = \boldsymbol{w}^0(\boldsymbol{x}), \quad \boldsymbol{x} \in \Omega \tag{2.23}$$

on the space $\boldsymbol{S}_h$. This means that $\Pi_h \boldsymbol{w}^0 \in \boldsymbol{S}_h$ and

$$(\Pi_h \boldsymbol{w}^0, \varphi_h)_h = (\boldsymbol{w}^0, \varphi_h) \quad \forall \varphi_h \in \boldsymbol{S}_h. \tag{2.24}$$

Moreover, we consider boundary conditions, but we shall discuss them later in Section (2.1.3). Setting $r = 0$ we obtain the finite volume method using piecewise constant approximations.

The numerical flux $\boldsymbol{H}$ is assumed to be (locally) Lipschitz-continuous, consistent, i.e.

$$\boldsymbol{H}(\boldsymbol{w}, \boldsymbol{w}, \boldsymbol{n}) = \sum_{s=1}^{2} \boldsymbol{f}_s(\boldsymbol{w}) n_s, \tag{2.25}$$

and conservative, i.e.

$$\boldsymbol{H}(\boldsymbol{u}, \boldsymbol{w}, \boldsymbol{n}) = -\boldsymbol{H}(\boldsymbol{w}, \boldsymbol{u}, -\boldsymbol{n}). \tag{2.26}$$

We choose the numerical flux with a convenient form for the semi-implicit linearization with respect to time. Particularly, this numerical flux can be written in the form

$$\boldsymbol{H}(\boldsymbol{w}_L, \boldsymbol{w}_R, \boldsymbol{n}) = \boldsymbol{A}_L(\boldsymbol{w}_L, \boldsymbol{w}_R, \boldsymbol{n}) \boldsymbol{w}_L + \boldsymbol{A}_R(\boldsymbol{w}_L, \boldsymbol{w}_R, \boldsymbol{n}) \boldsymbol{w}_R \tag{2.27}$$

with some matrices $\boldsymbol{A}_L, \ \boldsymbol{A}_R : \ I\!R^4 \times I\!R^4 \times I\!R^4 \to I\!R^{4\times 4}$.

In particular, we shall be concerned with the Vijayasundaram numerical flux $\boldsymbol{H}_{VS}$ (see [16]). We define *absolute value*, *positive part* and *negative part* of the matrix $\mathbb{P}$ with help of Lemma 2.1:

$$\begin{aligned} |\mathbb{P}|(\boldsymbol{w},\boldsymbol{n}) &= \mathbb{T}|\mathbb{\Lambda}|\mathbb{T}^{-1}, \\ \mathbb{P}^{\pm}(\boldsymbol{w},\boldsymbol{n}) &= \mathbb{T}\mathbb{\Lambda}^{\pm}\mathbb{T}^{-1}, \end{aligned} \tag{2.28}$$

where

$$\begin{aligned} |\mathbb{\Lambda}| &= \mathrm{diag}(|\lambda_1|,\ldots,|\lambda_4|), \\ \mathbb{\Lambda}^{\pm} &= \mathrm{diag}(\lambda_1^{\pm},\ldots,\lambda_4^{\pm}), \\ \lambda^{+} &= \max\{\lambda,0\}, \\ \lambda^{-} &= \min\{\lambda,0\}. \end{aligned} \tag{2.29}$$

Then we define the Vijayasundaram numerical flux $\boldsymbol{H}_{VS}$:

$$\boldsymbol{H}_{VS}(\boldsymbol{w}_L,\boldsymbol{w}_R,\boldsymbol{n}) = \mathbb{P}^{+}(\frac{\boldsymbol{w}_L+\boldsymbol{w}_R}{2},\boldsymbol{n})\boldsymbol{w}_L + \mathbb{P}^{-}(\frac{\boldsymbol{w}_L+\boldsymbol{w}_R}{2},\boldsymbol{n})\boldsymbol{w}_R. \tag{2.30}$$

For explicit formula for $\mathbb{T},\ \mathbb{D},\ \mathbb{T}^{-1}$ see [6]. The eigenvalues λ_i have the form

$$\begin{aligned} \lambda_1 =& \boldsymbol{v}\cdot\boldsymbol{n} - a, \\ \lambda_2 =& \lambda_3 = \boldsymbol{v}\cdot\boldsymbol{n}, \\ \lambda_4 =& \boldsymbol{v}\cdot\boldsymbol{n} + a, \end{aligned} \tag{2.31}$$

a is speed of sound (2.7).

2.1.2 Time discretization

Condition (2.21) is equivalent to a large system of ordinary differential equations. To solve this system we can apply several numerical schemes like Runge-Kutta schemes that are conditionally stable and the time step is strongly limited by the CFL-stability condition. This stability condition becomes very restrictive with increasing polynomial degree r of the discontinuous Galerkin space discretization. Further, the fully implicit backward Euler method can be use. This method leads to a large system of highly nonlinear algebraic equations, whose numerical solution is rather complicated. For these reasons we choose the semi-implicit scheme based on a suitable partial linearization of the form $\widetilde{b_h}$, which gives us a higher order unconditionally stable scheme.

We consider partition $0 = t_0 < t_1 < \ldots$ of the time interval $(0,T)$. We set $\tau_k = t_{k+1} - t_k$. We denote approximation of $\boldsymbol{w}(t_k)$ as $\boldsymbol{w}_h^k$. We use technique based on linearization of the form $\widetilde{b_h}$ carried out with the aid of the homogeneity of

the fluxes $\boldsymbol{f}_s$ and the use of the Vijayasundaram numerical flux (described in the previous section). In this way we obtain the form

$$b_h(\boldsymbol{w}_h^k,\varphi_h) = -\sum_{K_i\in T_h}\int_{K_i}\sum_{s=1}^{2}\boldsymbol{A}_s(\boldsymbol{w}_h^k(\boldsymbol{x}))\boldsymbol{w}_h^{k+1}(\boldsymbol{x})\cdot\frac{\partial\varphi_h}{\partial x_s}d\boldsymbol{x}$$
$$+\sum_{K_i\in T_h}\sum_{j\in S(i)}\int_{\Gamma_{ij}}\left(\mathbb{P}^+\left(\left\langle\boldsymbol{w}_h^k\right\rangle,\boldsymbol{n}_{ij}\right)\boldsymbol{w}_h^{k+1}|_{\Gamma_{ij}}+\mathbb{P}^-\left(\left\langle\boldsymbol{w}_h^k\right\rangle,\boldsymbol{n}_{ij}\right)\boldsymbol{w}_h^{k+1}|_{\Gamma_{ji}}\right)\cdot\varphi_h dS, \tag{2.32}$$

which is linear with respect to the second $\boldsymbol{w}_h^{k+1}$ and third φ_h argument. On the basis of the above considerations we obtain the following semi-implicit scheme: For each $k\geq 0$ find $\boldsymbol{w}_h^{k+1}$ such that

$$\boldsymbol{w}_h^{k+1}\in\mathbf{S}_h, \tag{2.33}$$

$$\left(\frac{\boldsymbol{w}_h^{k+1}-\boldsymbol{w}_h^k}{\tau},\varphi_h\right)_h + b_h(\boldsymbol{w}_h^k,\boldsymbol{w}_h^{k+1},\varphi_h)=0,\quad \forall\varphi_h\in\mathbf{S}_h,\ k=0,1,\ldots, \tag{2.34}$$

$$\boldsymbol{w}_h(0)=\Pi_h\boldsymbol{w}^0. \tag{2.35}$$

This is a first order accurate scheme in time. In the solution of nonstationary flows, it is necessary to apply a scheme, which is sufficiently accurate in space as well as in time. One possibility is to apply the following two step second order time discretization. We use second order approximation $\widetilde{\boldsymbol{w}}_h^{k+1}$ of $\boldsymbol{w}_h(t_{k+1})$ obtained by extrapolation

$$\widetilde{\boldsymbol{w}}_h^{k+1}=\frac{\tau_k+\tau_{k-1}}{\tau_{k-1}}\boldsymbol{w}_h^k-\frac{\tau_k}{\tau_{k-1}}\boldsymbol{w}_h^{k-1}, \tag{2.36}$$

which replaces the state $\boldsymbol{w}_h^k$ in the form b_h. Moreover, the second order backward difference approximation of the time derivative of the solution at t_{k+1} is used

$$\begin{aligned}\frac{\partial\boldsymbol{w}_h(\boldsymbol{x},t)}{\partial t}|_{t=t_{k+1}}&\approx\frac{2\tau_k+\tau_{k-1}}{\tau_k(\tau_k+\tau_{k-1})}\boldsymbol{w}_h(\boldsymbol{x},t_{k+1})\\ -\frac{\tau_k+\tau_{k-1}}{\tau_k\tau_{k-1}}\boldsymbol{w}_h(\boldsymbol{x},t_k)&+\frac{\tau_k}{\tau_{k-1}(\tau_k+\tau_{k-1})}\boldsymbol{w}_h(\boldsymbol{x},t_{k-1}).\end{aligned} \tag{2.37}$$

This leads to the following two step second-order scheme:
For each $k\geq 1$ find $\boldsymbol{w}_h^{k+1}$ such that

$$\boldsymbol{w}_h^{k+1}\in\mathbf{S}_h, \tag{2.38}$$

$$\begin{aligned}&\frac{2\tau_k+\tau_{k-1}}{\tau_k(\tau_k+\tau_{k-1})}\left(\boldsymbol{w}_h^{k+1},\varphi_h\right)_h+b_h(\widetilde{\boldsymbol{w}}_h^{k+1},\boldsymbol{w}_h^{k+1},\varphi_h)=\\ &=\frac{\tau_k+\tau_{k-1}}{\tau_k\tau_{k-1}}(\boldsymbol{w}_h^k,\varphi_h)_h-\frac{\tau_k}{\tau_{k-1}(\tau_k+\tau_{k-1})}(\boldsymbol{w}_h^{k-1},\varphi_h)_h,\\ &\qquad\forall\varphi_h\in\mathbf{S}_h,\ k=0,1,\ldots,\end{aligned} \tag{2.39}$$

$$\boldsymbol{w}_h(0) = \Pi_h \boldsymbol{w}^0. \tag{2.40}$$

We compute first time step $\boldsymbol{w}_h^1$ by the Runge-Kutta method. In order to guarantee the stability of the scheme, we use the CLF condition

$$\tau_k \max_{K_i \in T_h} \frac{1}{|K_i|} \left(\max_{j \in S_i} |\Gamma_{ij}| \, \lambda^{\max}_{\mathbb{P}(\boldsymbol{w}_h^k|_{\Gamma_{ij}}, \boldsymbol{n}_{ij})} \right) \leq CLF, \tag{2.41}$$

where $|K_i|$ denotes the area of K_i, Γ_{ij} the length of the edge Γ_{ij}, CFL is a given constant and $\lambda^{\max}_{\mathbb{P}(\boldsymbol{w}_h^k|_{\Gamma_{ij}}, \boldsymbol{n}_{ij})}$ is the maximal eigenvalue of the matrix $\mathbb{P}(\boldsymbol{w}_h^k|_{\Gamma_{ij}}, \boldsymbol{n}_{ij})$ where the maximum is taken over Γ_{ij}. This condition is a heuristic extension of a similar condition applied in the finite volume method (see, e.g. [6]).

2.1.3 Boundary conditions

If $\Gamma_{ij} \subset \partial\Omega_h$, i.e. $j \in \gamma(i)$, it is necessary to specify the boundary state $\boldsymbol{w}_h^{k+1}|_{\Gamma_{ji}}$ appearing in the numerical flux $\boldsymbol{H}$ in the definition of the inviscid form b_h.

On $\Gamma = \Gamma_{ij} \subset \Gamma_W$, i.e. solid impermeable wall with normal $\boldsymbol{n} = \boldsymbol{n}_{ij}$, we prescribe so-called *no-stick* condition

$$\boldsymbol{v} \cdot \boldsymbol{n} = 0 \text{ on } \Gamma. \tag{2.42}$$

We use the approximation

$$\int_{\Gamma_{ij}} \boldsymbol{H}(\boldsymbol{w}_h^{k+1}|_{\Gamma_{ij}}, \boldsymbol{w}_h^{k+1}|_{\Gamma_{ji}}, \boldsymbol{n}_{ij}) \cdot \varphi_h dS \approx \int_{\Gamma_{ij}} \mathbf{F}_W(\boldsymbol{w}_h^k, \boldsymbol{w}_h^{k+1}, \boldsymbol{n}_{ij}) \cdot \varphi_h dS \tag{2.43}$$

where

$$\mathbf{F}_W(\boldsymbol{w}_h^k, \boldsymbol{w}_h^{k+1}, \boldsymbol{n}) = \frac{D\mathcal{P}}{D\boldsymbol{w}}(\boldsymbol{w}_h^k, \boldsymbol{n}) \boldsymbol{w}_h^{k+1} = \mathbb{P}(\boldsymbol{w}_h^k, \boldsymbol{n}) \boldsymbol{w}_h^{k+1}. \tag{2.44}$$

Taking into account the no-stick condition on the impermeable wall, the normal component of the inviscid flux has the form

$$\mathcal{P}(\boldsymbol{w}, \boldsymbol{n}) = \sum_{s=1}^{2} \boldsymbol{f}_s(\boldsymbol{w}) n_s = (\boldsymbol{v} \cdot \boldsymbol{n}) + p(0, n_1, n_2, \boldsymbol{v} \cdot \boldsymbol{n})^T = p(0, n_1, n_2, 0)^T. \tag{2.45}$$

If we extrapolate the value of the pressure by $p_R = p_L$, we can define the numerical flux

$$\boldsymbol{H}(\boldsymbol{w}_L, \boldsymbol{w}_R, \boldsymbol{n}) = p(0, n_1, n_2, 0)^T. \tag{2.46}$$

In the case of the inlet and outlet conditions there is a problem, which quantities should be prescribed (Dirichlet condition) and which should be extrapolated onto Γ from the adjacent element (Neumann-type condition). One possibility used often in practice is given in [6] using the method of characteristics. We use and describe here an another way.

Let $\Gamma = \Gamma_{ij} \subset \Gamma_{IO}$ and $\boldsymbol{n} = \boldsymbol{n}_{ij}$ be the outer unit normal to K_i on Γ. In order to compute $\boldsymbol{H}(\boldsymbol{w}_i, \boldsymbol{w}_j, \boldsymbol{n})$, we need to specify the value $\boldsymbol{w}_j$ when $\boldsymbol{w}_i$ is known.

Let us introduce a new Cartesian coordinate system $\tilde{x}_1, \tilde{x}_2$ in $I\!R^2$ with the origin at the center of gravity of the edge Γ, the coordinates $\tilde{x}_1, \tilde{x}_2$ are oriented in the direction of normal $\boldsymbol{n}$ and tangent to Γ, respectively. The Euler equations transformed into this new coordinate system have the form

$$\frac{\partial \boldsymbol{q}}{\partial t} + \sum_{s=1}^{2} \frac{\partial \boldsymbol{f}_s(\boldsymbol{q})}{\partial \tilde{x}_s} = 0, \tag{2.47}$$

as follows from the rotational invariance of the Euler equations. Here

$$\boldsymbol{q} = \mathbb{Q}(\boldsymbol{n})\boldsymbol{w}, \tag{2.48}$$

where

$$\mathbb{Q}(\boldsymbol{n}) = \begin{pmatrix} 1 & 0 & 0 & 0 \\ 0 & n_1 & n_2 & 0 \\ 0 & -n_2 & n_1 & 0 \\ 0 & 0 & 0 & 1 \end{pmatrix}.$$

Now we neglect the tangential derivative $\partial/\partial\tilde{x}_2$ and get the system with one space variable $\tilde{x}_1$ in the form

$$\frac{\partial \boldsymbol{q}}{\partial t} + \frac{\partial \boldsymbol{f}_1(\boldsymbol{q})}{\partial \tilde{x}_1} = 0. \tag{2.49}$$

Using the homogeneity (2.5) of the fluxes we can write the above equation in the nonconservative form

$$\frac{\partial \boldsymbol{q}}{\partial t} + \mathbb{A}_1(\boldsymbol{q})\frac{\partial \boldsymbol{q}}{\partial \tilde{x}_1} = 0. \tag{2.50}$$

Finally we linearize this system around the state $\boldsymbol{q}_i = \mathbb{Q}(\boldsymbol{n})\boldsymbol{w}_i$ and obtain the linear system

$$\frac{\partial \boldsymbol{q}}{\partial t} + \mathbb{A}_1(\boldsymbol{q}_i)\frac{\partial \boldsymbol{q}}{\partial \tilde{x}_1} = 0, \tag{2.51}$$

which will be considered in the set $(-\infty, 0) \times (0, \infty)$ and equipped with the initial condition

$$\boldsymbol{q}(\tilde{x}_1, 0) = \boldsymbol{q}_i, \quad \tilde{x}_1 \in (-\infty, 0) \tag{2.52}$$

and the boundary condition

$$\boldsymbol{q}(0, t) = \boldsymbol{q}_j, \quad t > 0. \tag{2.53}$$

The goal is to choose $\boldsymbol{q}_j$ in such a way that the initial-boundary value problem (2.51) - (2.53) has a unique solution. The solution can be written in the form

$$\boldsymbol{q}(\tilde{x}_1, t) = \sum_{s=1}^{4} \mu(\tilde{x}_1, t)\boldsymbol{r}_s, \tag{2.54}$$

where $\boldsymbol{r}_s = \boldsymbol{r}_s(\boldsymbol{q}_i)$ are the eigenvectors of the matrix $\mathbb{A}_1(\boldsymbol{q}_i)$ corresponding to its eigenvalues $\tilde{\lambda}_s = \tilde{\lambda}_s(\boldsymbol{q}_i)$ and creating a basis in $I\!R^4$. Moreover,

$$\boldsymbol{q}_i = \sum_{s=1}^{4} \alpha_s \boldsymbol{r}_s, \quad \boldsymbol{q}_j = \sum_{s=1}^{4} \beta_s \boldsymbol{r}_s. \tag{2.55}$$

Substituting (2.54) into (2.51) and using the relation $\mathbb{A}_1(\boldsymbol{q}_i)\boldsymbol{r}_s = \tilde{\lambda}_s \boldsymbol{r}_s$, we find out that problem (2.51 - 2.53) is equivalent to 4 mutually independent linear initial-boundary value scalar problems for $s = 1; \ldots; 4$:

$$\begin{aligned} \frac{\partial \mu_s}{\partial t} + \tilde{\lambda}_s \frac{\partial \mu_s}{\partial \tilde{x}_1} = 0 \quad &\text{in} \quad (-\infty, 0) \times (0, \infty), \\ \mu_s(\tilde{x}_1, 0) = \alpha_s, \quad &\tilde{x}_1 \in (-\infty, 0), \\ \mu_s(0, t) = \beta_s, \quad &t \in (0, \infty). \end{aligned} \tag{2.56}$$

This can be solved by the method of characteristics. The solution is

$$\mu_s(\tilde{x}_1, t) = \begin{cases} \alpha_s, & \tilde{x}_1 - \tilde{\lambda}_s t < 0, \\ \beta_s, & \tilde{x}_1 - \tilde{\lambda}_s t > 0. \end{cases}$$

Conclusion:

- $\tilde{\lambda}_s > 0$, then $\beta_s = \alpha_s$ (β_s is not prescribed, but obtained by the extrapolation of μ_s to the boundary $\tilde{x}_1 = 0$),
- $\tilde{\lambda}_s = 0$, then β_s is not prescribed, but can be defined as $\beta_s = \alpha_s$ by the continuous extension of μ_s to the boundary $\tilde{x}_1 = 0$,
- $\tilde{\lambda}_s < 0$, then β_s must be prescribed.

Furthermore, we incorporate the fact that

$$\tilde{\lambda}_s(\boldsymbol{q}_i) = \lambda_s(\boldsymbol{w}_i, \boldsymbol{n}), \quad s = 1, \ldots, 4, \tag{2.57}$$

where $\lambda_s(\boldsymbol{w}_i, \boldsymbol{n})$ are the eigenvalues of the Jacobi matrix $\mathbb{P}(\boldsymbol{w}_i, \boldsymbol{n})$. We come to the conclusion, that we prescribe n_{pr} quantities characterizing $\boldsymbol{w}$, where n_{pr} is the number of negative eigenvalues λ_s, and extrapolate $n_{ex} = 4 - n_{pr}$ quantities. We propose to prescribe variables based on the local linearized problem.

We shall put $\boldsymbol{q}_j^0 = \mathbb{Q}(\boldsymbol{n})\boldsymbol{w}_j^0$, where $\boldsymbol{w}_j^0$ is a prescribed state depending on the situation and interpretation. This state and above results will allow us to determine the sought boundary state $\boldsymbol{w}_j$. We express the state $\boldsymbol{q}_j^0$ in the form

$$\boldsymbol{q}_j^0 = \sum_{s=1}^{4} \gamma_s \boldsymbol{r}_s \tag{2.58}$$

and denote by $\mathbb{T}$ the matrix, which has the $\boldsymbol{r}_s$ for its columns. We set $\beta = (\beta_1, \ldots, \beta_4)^T$ and $\gamma = (\gamma_1, \ldots, \gamma_4)^T$ and write

$$\begin{aligned} \boldsymbol{q}_i &= \mathbb{T}\alpha \Leftrightarrow \alpha = \mathbb{T}^{-1}\boldsymbol{q}_i, \\ \boldsymbol{q}_j^0 &= \mathbb{T}\gamma \Leftrightarrow \gamma = \mathbb{T}^{-1}\boldsymbol{q}_j^0. \end{aligned} \tag{2.59}$$

Now we calculate the state $\boldsymbol{q}_j$ according to the presented process

$$\boldsymbol{q}_j := \sum_{s=1}^{4} \beta_s \boldsymbol{r}_s = \mathbb{T}\beta, \tag{2.60}$$

where

$$\beta_s = \begin{cases} \alpha_s, & \lambda_s \geq 0, \\ \gamma_s, & \lambda_s < 0. \end{cases}$$

Finally $\boldsymbol{w}_j = \mathbb{Q}^{-1}(\boldsymbol{n})\boldsymbol{q}_j$ and we can use this to calculate $\boldsymbol{H}(\boldsymbol{w}_i, \boldsymbol{w}_j, \boldsymbol{n})$. In the framework of the presented theory, these boundary conditions seem to give the natural choice for $\boldsymbol{w}_j$. However, we must keep in mind two simplifications that we have made during the derivation:

- We have neglected tangential derivatives of the solution in order to get a simplified equation (2.49).
- We have avoided the nonlinearity of problem by local linearization (2.51).

Nonetheless, experiments show that this method applied to the approximation of inlet and outlet boundary conditions lets density and pressure waves pass through the boundaries without reflection.

2.1.4 Shock capturing

For high-speed flow with shock waves and contact discontinuities it is necessary to avoid the Gibbs phenomenon manifested by spurious overshoots and undershoots in computed quantities near discontinuities and steep gradients. In this case these phenomena cause instabilities in the semi-implicit solution. One possibility for avoiding the Gibbs phenomenon is the use of the limiting of order of accuracy of the method in the vicinity of discontinuities. The limiting technique is motivated by the paper [1], on the basis of which the left-hand

side of (2.34) and (2.39) is augmented by an artificial viscosity form. However, since this form is nonzero also in regions where the exact solution is regular, a small nonphysical entropy production can appear in these regions. Therefore, this technique is combined with the approach proposed in [5]. It is based on the discontinuity indicator $g^k(i)$ defined by

$$g^k(i) = \int_{\partial K_i} [\rho_h^k]^2 dS/(h_{K_i}|K_i|^{3/4}), \quad K_i \in T_h. \tag{2.61}$$

By $[\rho_h^k]$ we denote the jump of the density on ∂K_i at time instant t. The indicator $g^k(i)$ was constructed in such a way that it takes an anisotropy of the computational mesh into account. Now we introduce the discrete discontinuity indicator

$$\begin{aligned} G^k(i) &= 0 \quad \text{if } g^k(i) < 1,\ K_i \in T_h, \\ G^k(i) &= 1 \quad \text{if } g^k(i) \geq 1,\ K_i \in T_h, \end{aligned} \tag{2.62}$$

and add the artificial viscosity form

$$\beta(\boldsymbol{w}_h^k, \boldsymbol{w}_h^{k+1}, \varphi) = \nu_1 \sum_{i \in I} h_{K_i} G^k(i) \int_{K_i} \nabla \boldsymbol{w}_h^{k+1} \cdot \nabla \varphi d\boldsymbol{x} \tag{2.63}$$

with $\nu_1 = O(1)$ to the left-hand side of (2.34) and (2.39). Since the artificial viscosity form is rather local, it is proposed to augment the left-hand side of (2.34) and (2.39) by adding the form

$$J_h(\boldsymbol{w}_h^k, \boldsymbol{w}_h^{k+1}, \varphi) = \nu_2 \sum_{i \in I} \sum_{j \in s(i)} \frac{1}{2}(G^k(i) + G^k(j)) \int_{\Gamma_{ij}} [\boldsymbol{w}_h^{k+1}] \cdot [\varphi] dS, \tag{2.64}$$

where $\nu_2 = O(1)$, which allows to strengthen the influence of neighboring elements and improves the behavior of the method. Thus, the resulting scheme obtained by limiting of (2.34) is

$$\boldsymbol{w}_h^{k+1} \in \mathbf{S}_h, \tag{2.65}$$

$$\begin{aligned} \left(\frac{\boldsymbol{w}_h^{k+1} - \boldsymbol{w}_h^k}{\tau}, \varphi_h \right)_h + b_h(\boldsymbol{w}_h^k, \boldsymbol{w}_h^{k+1}, \varphi_h) + J_h(\boldsymbol{w}_h^k, \boldsymbol{w}_h^{k+1}, \varphi) \\ + \beta(\boldsymbol{w}_h^k, \boldsymbol{w}_h^{k+1}, \varphi) = 0, \quad \forall \varphi_h \in \mathbf{S}_h,\ k = 0, 1, \ldots, \end{aligned} \tag{2.66}$$

$$\boldsymbol{w}_h(0) = \Pi_h \boldsymbol{w}^0. \tag{2.67}$$

Similarly, we obtained a stabilized version of the scheme (2.39). The same stabilization technique can be used easily in the problem of time-dependent domain, which will be treated later.

2.2 Time-dependent domain

In this section we shall describe Arbitrary Eulerian-Lagrangian (ALE) method ([2], [15], [14], [13]) and discretization of the ALE formulation of the Euler equations.

2.2.1 ALE method for Euler equations

We assume that (0,T) with $T > 0$ is a time interval and by Ω_t we denote a computational domain occupied by the fluid at time t. $\mathcal{M} = \{(\boldsymbol{x}, t);\ \boldsymbol{x} \in \Omega_t,\ t \in (0, T)\}$ will be called the space-time cylinder. We denote $\Omega_{ref} = \Omega_0$ the domain at the initial time. We call it the *reference configuration*. A smooth,
one-to-one mapping of the reference configuration onto the computational domain Ω_t at time t (*current configuration*) is denoted by $\mathcal{A}_t$, i.e.

$$\begin{aligned} \mathcal{A}_t &: \bar{\Omega}_{ref} \to \bar{\Omega}_t, \\ \boldsymbol{X} &\mapsto \boldsymbol{x}(\boldsymbol{X}, t) = \mathcal{A}_t(\boldsymbol{X}). \end{aligned} \tag{2.68}$$

We define the *domain velocity* $\tilde{\boldsymbol{z}}$ at all points $\boldsymbol{X}$ of the reference configuration Ω_{ref} for each time level

$$\begin{aligned} \tilde{\boldsymbol{z}} &: \bar{\Omega}_{ref} \times (0, T) \to I\!R^2, \\ \tilde{\boldsymbol{z}}(\boldsymbol{X}, t) &= \frac{\partial}{\partial t}\boldsymbol{x}(\boldsymbol{X}, t) = \frac{\partial}{\partial t}\mathcal{A}(\boldsymbol{X}). \end{aligned} \tag{2.69}$$

We can transform the domain velocity to space coordinates $\boldsymbol{x}$ by the relation

$$\boldsymbol{z} = \tilde{\boldsymbol{z}}(\mathcal{A}_t^{-1}(\boldsymbol{x}), t),\ t \in (0, T),\ \boldsymbol{x} \in \bar{\Omega}_t. \tag{2.70}$$

We further introduce the so-called *ALE derivative* $\frac{D^{\mathcal{A}}}{Dt}$ for a function $f = f(\boldsymbol{x}, t),\ \boldsymbol{x} \in \Omega_t,\ t \in (0, t)$. We set

$$\frac{D^{\mathcal{A}}}{Dt} f(\boldsymbol{x}, t) = \frac{\partial \tilde{f}}{\partial t}(\boldsymbol{X}, t), \quad \boldsymbol{X} = \mathcal{A}_t^{-1}(\boldsymbol{x}), \tag{2.71}$$

where $\tilde{f}(\boldsymbol{X}, t) = f(\mathcal{A}_t(\boldsymbol{X}), t),\ \boldsymbol{X} \in \Omega_{ref},\ t \in (0, T)$. If we assume that the function f is continuously differentiable and use the chain rule, we find that

$$\begin{aligned} \frac{D^{\mathcal{A}}}{Dt} f &= \frac{\partial f}{\partial t} + (\boldsymbol{z} \cdot \nabla) f, \\ \frac{D^{\mathcal{A}}}{Dt} f &= \frac{\partial f}{\partial t} + \operatorname{div}(f\boldsymbol{z}) - f(\boldsymbol{z}). \end{aligned} \tag{2.72}$$

This means

$$\frac{\partial f}{\partial t} = \frac{D^{\mathcal{A}}}{Dt} f - (\boldsymbol{z} \cdot \nabla) f, \tag{2.73}$$

$$\frac{\partial f}{\partial t} = \frac{D^{\mathcal{A}}}{Dt} f - \operatorname{div}(f\boldsymbol{z}) + f(\boldsymbol{z}). \tag{2.74}$$

Using the relation (2.74), we obtain the Euler equations in the form

$$\frac{D^{\mathcal{A}}\boldsymbol{w}}{Dt} + \sum_{s=1}^{2} \frac{\partial \boldsymbol{g}_s(\boldsymbol{w})}{x_s} + \boldsymbol{w}\,\mathrm{div}\boldsymbol{z} = 0 \quad \text{in } Q_t, \tag{2.75}$$

where $\boldsymbol{g}_s,\ s = 1, 2$, is the ALE flux of $\boldsymbol{w}$ in the direction x_s defined as

$$g_s(\boldsymbol{w}) = f_s(\boldsymbol{w}) - z_s\boldsymbol{w}. \tag{2.76}$$

2.2.2 Discretization of the ALE formulation

We use notation described in Section (2.1.1). By Ω_{ht} we further denote a polygonal approximation of Ω_t at time t and by T_{ht} we denote a partition of Ω_{ht}. T_{ht} is a set of triangles $K_i,\ i \in I_t$.

The approximate solution will be sought at each time instant t as an element of the finite-dimensional space

$$\mathbf{S}_{ht} = \mathbf{S}^{r,-1}(\Omega_{ht}, T_{ht}) = \{\varphi_h;\ \varphi_h|_K \in P^r(K)\ \forall K \in T_{ht}\}^4. \tag{2.77}$$

We multiply (2.75) by a test function $\varphi \in S_{ht}$, integrate over any element K_i, apply Green's theorem and sum over all $i \in I_t$:

$$\begin{aligned}\sum_{K_i\in T_{ht}} \int_{K_i} \frac{D^{\mathcal{A}}\boldsymbol{w}(t)}{Dt}\cdot\varphi d\boldsymbol{x} &= \sum_{K_i\in T_{ht}} \int_{K_i} \sum_{s=1}^{2} g_s(\boldsymbol{w}(t))\cdot\frac{\partial\varphi}{\partial x_s} d\boldsymbol{x} \\ - \sum_{K_i\in T_{ht}} \sum_{j\in S_t(i)} \int_{K_i} \sum_{s=1}^{2} g_s(\boldsymbol{w}(t))(n_{ij})_s\cdot\varphi dS &- \sum_{K_i\in T_{ht}} \int_{K_i} \mathrm{div}\boldsymbol{z}(\boldsymbol{w}\cdot\varphi) d\boldsymbol{x}.\end{aligned} \tag{2.78}$$

We apply again the approximation of fluxes through the face Γ_{ij} by a numerical flux $\boldsymbol{H} = \boldsymbol{H}(\boldsymbol{u}, \boldsymbol{w}, \boldsymbol{n})$. It means that

$$\int_{\Gamma_{ij}} \sum_{s=1}^{2} g_s(\boldsymbol{w})(n_{ij})_s\cdot\varphi dS \approx \int_{\Gamma_{ij}} \boldsymbol{H}_g(\boldsymbol{w}_h|_{\Gamma_{ij}}, \boldsymbol{w}_h|_{\Gamma_{ji}}, \boldsymbol{n}_{ij})\cdot\varphi dS. \tag{2.79}$$

By $\boldsymbol{H}_g$ we denote analogy of Vijayasundaram numerical flux consistent with the fluxes $g_s,\ s = 1, 2$. We have

$$\frac{Dg_s(\boldsymbol{w})}{D\boldsymbol{w}} = \frac{Df_s(\boldsymbol{w})}{D\boldsymbol{w}} - z_s\mathbb{I} = \mathbb{A}_s - z_s\mathbb{I}. \tag{2.80}$$

Hence

$$\tilde{\mathbb{P}}(\boldsymbol{w}, \boldsymbol{n}) = \sum_{s=1}^{2} \frac{Dg_s(\boldsymbol{w})}{D\boldsymbol{w}} n_s = \sum_{s=1}^{2} \mathbb{A}_s n_s - z_s n_s \mathbb{I} = \mathbb{P}(\boldsymbol{w}, \boldsymbol{n}) - (\boldsymbol{z}\cdot\boldsymbol{n})\mathbb{I}. \tag{2.81}$$

We continue similarly as in (2.28) and (2.29) and write

$$\tilde{\mathbb{P}} = \mathbb{T}\tilde{\mathbb{A}}\mathbb{T}^{-1} \text{ with } \tilde{\mathbb{A}} = \text{diag}(\lambda_1 - \boldsymbol{z}\cdot\boldsymbol{n}, \lambda_2 - \boldsymbol{z}\cdot\boldsymbol{n}, \lambda_3 - \boldsymbol{z}\cdot\boldsymbol{n}, \lambda_4 - \boldsymbol{z}\cdot\boldsymbol{n}). \quad (2.82)$$

We define $\tilde{\mathbb{P}}^+$ and $\tilde{\mathbb{P}}^-$ in the same way as in (2.28). We now define modified Vijayasundaram numerical flux

$$\boldsymbol{H}_g(\boldsymbol{w}_L, \boldsymbol{w}_R, \boldsymbol{n}) = \tilde{\mathbb{P}}^+(\frac{\boldsymbol{w}_L + \boldsymbol{w}_R}{2}, \boldsymbol{n})\boldsymbol{w}_L + \tilde{\mathbb{P}}^-(\frac{\boldsymbol{w}_L + \boldsymbol{w}_R}{2}, \boldsymbol{n})\boldsymbol{w}_R. \quad (2.83)$$

We define the forms

$$(\frac{D^{\mathcal{A}}\boldsymbol{w}_h(t)}{Dt}, \varphi_h)_h = \int_{\Omega_{ht}} \frac{D^{\mathcal{A}}\boldsymbol{w}_h(t)}{Dt}\cdot\varphi_h d\boldsymbol{x}, \quad (2.84)$$

$$\tilde{b}_h^2(\boldsymbol{w}_h(t), \varphi_h) = -\sum_{K_i\in T_{ht}} \int_{K_i} \sum_{s=1}^{2} g_s(\boldsymbol{w}(t))\cdot\frac{\partial\varphi}{\partial x_s} d\boldsymbol{x} \quad (2.85)$$

$$+ \sum_{K_i\in T_{ht}} \sum_{j\in S_t(i)} \int_{\Gamma_{ij}} \boldsymbol{H}_g(\boldsymbol{w}_h(t)|_{\Gamma_{ij}}, \boldsymbol{w}_h(t)|_{\Gamma_{ji}}, \boldsymbol{n}_{ij})\cdot\varphi dS,$$

$$d_h^2(\boldsymbol{w}_h(t), \varphi_h) = -\sum_{K_i\in T_{ht}} \text{div}\boldsymbol{z}(\boldsymbol{w}_h(t)\cdot\varphi) d\boldsymbol{x}. \quad (2.86)$$

Chapter 3

DGFEM discretization of the Navier-Stokes equations in time-dependent domains

We shall describe DGFE discretization of equations describing compressible viscous flow in time-dependent domains. We will employ some procedures used in the discretization of the Euler equations.

3.1 Continuous problem

We consider the system of equations consisting of the continuity equation, the compressible Navier-Stokes equations and the energy equation. All these equations are presented in Chapter 1. To this system we add thermodynamical relations from Section 1.7. Further, we define as in Chapter 2 disjoint boundary components Γ_I, Γ_O, Γ_W, the *inlet*, *outlet* and *impermeable wall* respectively, $\Gamma_I \cup \Gamma_O \cup \Gamma_W = \partial\Omega$. Next we set $\Gamma_{IO} = \Gamma_I \cup \Gamma_O$. The system of equations reads

$$\frac{\partial \boldsymbol{w}}{\partial t} + \sum_{s=1}^{2} \frac{\partial \boldsymbol{f}_s(\boldsymbol{w})}{\partial x_s} = \sum_{s=1}^{2} \frac{\partial (R)_s(\boldsymbol{w}, \nabla, \boldsymbol{w})}{\partial x_s} + \boldsymbol{F}(\boldsymbol{w}) \quad \text{in } Q_T, \tag{3.1}$$

where $Q_T = \Omega \times (0,T),\ \Omega \subset I\!R^2,\ T > 0$, $\boldsymbol{w}(x,t)$ is the state vector, $\boldsymbol{f}_1, \boldsymbol{f}_2$ are the inviscid fluxes and $(R)_1$, $(R)_2$ are viscous fluxes:

$$\begin{aligned}
\boldsymbol{w} =&(\rho, \rho v_1, \rho v_2, E)^T \in I\!R^4,\\
\boldsymbol{f}_i(\boldsymbol{w}) =&(f_{i1}(\boldsymbol{w}), \ldots, f_{i4}(\boldsymbol{w}))\\
=&(\rho v_i, \rho v_1 v_i + \delta_{1i} p, \rho v_2 v_i + \delta_{2i} p, (E+p)v_i)^T,\\
(R)(\boldsymbol{w}, \nabla \boldsymbol{w}) =&(0, \tau_{i1}, \tau_{i2}, \tau_{i1} v_1 + \tau_{i2} v_2 + k\frac{\partial \theta}{\partial x_i})^T,\\
\tau_{ij} =&\lambda \delta_{ij} \mathrm{div} \boldsymbol{v} + 2\mu d_{ij}(\boldsymbol{v}), \quad d_{ij}(\boldsymbol{v}) = \frac{1}{2}(\frac{\partial v_i}{\partial x_j} + \frac{\partial v_j}{\partial x_i}),\\
\boldsymbol{F}(\boldsymbol{w}) =&\rho(0, f_1, f_2, q)^T.
\end{aligned} \tag{3.2}$$

We add the thermodynamical relations

$$p = (\gamma - 1)(E - \rho|\boldsymbol{v}|^2/2) \tag{3.3}$$

and

$$\theta = \left(\frac{E}{\rho} - \frac{1}{2}|\boldsymbol{v}|^2\right)/c_v. \tag{3.4}$$

The notation here is the same as in Chapter 1. We prescribe initial condition

$$\boldsymbol{w}(x,0) = \boldsymbol{w}_0(x) \quad x \in \Omega \tag{3.5}$$

and system of equations is completed with the following set of boundary conditions on appropriate parts of the boundary:

$$\begin{aligned}
&\text{Case } \Gamma_I:\\
&\qquad a)\ \rho|_{\Gamma_I \times (0,T)} = \rho_D,\\
&\qquad b)\ \boldsymbol{v}|_{\Gamma_I \times (0,T)} = \boldsymbol{v}_D,\\
&\qquad c)\ \sum_{j=1}^{2}\left(\sum_{i=1}^{2} \tau_{ij} n_i\right) v_j + k\frac{\partial \theta}{\partial \boldsymbol{n}} = 0 \text{ on } \Gamma_I \times (0,T);\\
&\text{Case } \Gamma_W:\\
&\qquad a)\ \boldsymbol{v}|_{\Gamma_W \times (0,T)} = \boldsymbol{z}_D = \text{velocity of moving wall},\\
&\qquad b)\ \frac{\partial \theta}{\partial \boldsymbol{n}} = 0 \text{ on } \Gamma_W \times (0,T);\\
&\text{Case } \Gamma_O:\\
&\qquad a)\ \sum_{i=1}^{2} \tau_{ij} n_i = 0,\ j = 1,2,\\
&\qquad b)\ \frac{\partial \theta}{\partial \boldsymbol{n}} = 0 \text{ on } \Gamma_W \times (0,T);
\end{aligned} \tag{3.6}$$

We use ALE method in the same way as described in Section 2.2.1. Following the procedure, we arrive to the ALE formulation of the Navier-Stokes equations

$$\frac{D^A \boldsymbol{w}}{Dt} + \sum_{s=1}^{2} \frac{\partial \boldsymbol{g}_s(\boldsymbol{w})}{\partial x_s} + \boldsymbol{w}\,\mathrm{div}\,\boldsymbol{z} = \sum_{s=1}^{2} \frac{\partial (R)_s(\boldsymbol{w}, \nabla \boldsymbol{w})}{\partial x_s}, \tag{3.7}$$

where

$$\boldsymbol{g}_s(\boldsymbol{w}) := \boldsymbol{f}_s(\boldsymbol{w}) - z_s \boldsymbol{w}, \quad s = 1, 2$$

are the ALE modified inviscid fluxes. The space and the time discretization is described as in [9].

3.2 Discrete problem

3.2.1 Discontinuous Galerkin space semidiscretization

We use the discontinuous Galerkin finite element method for the space semidiscretization. We construct a polygonal approximation Ω_{ht} of the domain Ω_t. By $\mathcal{T}_{ht}$ we denote a partition of the closure $\overline{\Omega}_{ht}$ of the domain Ω_{ht} into a finite number of closed triangles K with mutually disjoint interiors such that $\overline{\Omega}_{ht} = \bigcup_{K \in \mathcal{T}_{ht}} K$.

By $\mathcal{F}_{ht}$ we denote the system of all faces of all elements $K \in \mathcal{T}_{ht}$. Further, we introduce the set of all interior faces $\mathcal{F}_{ht}^I = \{\Gamma \in \mathcal{F}_{ht};\ \Gamma \subset \Omega\}$, the set of all boundary faces $\mathcal{F}_{ht}^B = \{\Gamma \in \mathcal{F}_{ht};\ \Gamma \subset \partial\Omega_{ht}\}$ and the set of all "Dirichlet" boundary faces $\mathcal{F}_{ht}^D = \left\{\Gamma \in \mathcal{F}_{ht}^B;\ \text{a Dirichlet condition is prescribed on } \Gamma\right\}$. Each $\Gamma \in \mathcal{F}_{ht}$ is associated with a unit normal vector $\boldsymbol{n}_\Gamma$ to Γ. For $\Gamma \in \mathcal{F}_{ht}^B$ the normal $\boldsymbol{n}_\Gamma$ has the same orientation as the outer normal to $\partial\Omega_{ht}$. We set $d(\Gamma) =$ length of $\Gamma \in \mathcal{F}_{ht}$.

For each $\Gamma \in \mathcal{F}_{ht}^I$ there exist two neighboring elements $K_\Gamma^{(L)}, K_\Gamma^{(R)} \in \mathcal{T}_h$ such that $\Gamma \subset \partial K_\Gamma^{(R)} \cap \partial K_\Gamma^{(L)}$. We use the convention that $K_\Gamma^{(R)}$ lies in the direction of $\boldsymbol{n}_\Gamma$ and $K_\Gamma^{(L)}$ lies in the opposite direction to $\boldsymbol{n}_\Gamma$. The elements $K_\Gamma^{(L)}$, $K_\Gamma^{(R)}$ are called neighbors. If $\Gamma \in \mathcal{F}_{ht}^B$, then the element adjacent to Γ will be denoted by $K_\Gamma^{(L)}$.

The approximate solution will be sought in the space of discontinuous piecewise polynomial functions

$$\boldsymbol{S}_{ht} = [S_{ht}]^4, \quad \text{with} \quad S_{ht} = \{v; v|_K \in P_r(K)\ \forall\, K \in \mathcal{T}_{ht}\}, \tag{3.8}$$

where $r \geq 0$ is an integer and $P_r(K)$ denotes the space of all polynomials on K of degree $\leq r$. A function $\boldsymbol{\varphi} \in \boldsymbol{S}_{ht}$ is, in general, discontinuous on interfaces $\Gamma \in \mathcal{F}_{ht}^I$. By $\boldsymbol{\varphi}_\Gamma^{(L)}$ and $\boldsymbol{\varphi}_\Gamma^{(R)}$ we denote the values of $\boldsymbol{\varphi}$ on Γ considered from the interior and the exterior of $K_\Gamma^{(L)}$, respectively, and set $\langle \boldsymbol{\varphi} \rangle_\Gamma = (\boldsymbol{\varphi}_\Gamma^{(L)} + \boldsymbol{\varphi}_\Gamma^{(R)})/2$, $[\boldsymbol{\varphi}]_\Gamma = \boldsymbol{\varphi}_\Gamma^{(L)} - \boldsymbol{\varphi}_\Gamma^{(R)}$.

Next, we multiply system (3.7) by a test function $\boldsymbol{\varphi}_h \in \boldsymbol{S}_{ht}$, integrate over $K \in \mathcal{T}_{ht}$, use Green's theorem, sum over all elements $K \in \mathcal{T}_{ht}$ and introduce the concept of the numerical flux and suitable terms mutually vanishing for a regular exact solution.
In this way we get the following identity:

$$\sum_{K\in\mathcal{T}_{ht}} \int_K \frac{D^A \boldsymbol{w}}{Dt} \cdot \boldsymbol{\varphi}_h \, dx + b_h(\boldsymbol{w}, \boldsymbol{\varphi}_h) + a_h(\boldsymbol{w}, \boldsymbol{\varphi}_h) + \tag{3.9}$$
$$J_h(\boldsymbol{w}, \boldsymbol{\varphi}_h) + d_h \boldsymbol{w}, \boldsymbol{\varphi}) = \ell_h(\boldsymbol{w}, \boldsymbol{\varphi}_h).$$

Here

$$\begin{aligned} b_h(\boldsymbol{w}, \boldsymbol{\varphi}_h) = &- \sum_{K\in\mathcal{T}_{ht}} \int_K \sum_{s=1}^{2} \boldsymbol{g}_s(\boldsymbol{w}) \cdot \frac{\partial \boldsymbol{\varphi}_h}{\partial x_s} \, dx \\ &+ \sum_{\Gamma\in\mathcal{F}_{ht}^I} \int_\Gamma \mathbf{H}_g(\boldsymbol{w}_\Gamma^{(L)}, \boldsymbol{w}_\Gamma^{(R)}, \boldsymbol{n}_\Gamma) \cdot [\boldsymbol{\varphi}_h]_\Gamma \, dS \\ &+ \sum_{\Gamma\in\mathcal{F}_{ht}^B} \int_\Gamma \mathbf{H}_g(\boldsymbol{w}_\Gamma^{(L)}, \boldsymbol{w}_\Gamma^{(R)}, \boldsymbol{n}_\Gamma) \cdot \boldsymbol{\varphi}_{h\Gamma}^{(L)} \, dS \end{aligned} \tag{3.10}$$

is the convection form, defined with the aid of a numerical flux $\mathbf{H}_g$. We require that it is consistent with the fluxes $\boldsymbol{g}_s$: $\mathbf{H}_g(\boldsymbol{w}, \boldsymbol{w}, \boldsymbol{n}) = \sum_{s=1}^{2} \boldsymbol{g}_s(\boldsymbol{w}) n_s$ $(\boldsymbol{n} = (n_1, n_2), |\boldsymbol{n}| = 1)$, conservative: $\mathbf{H}_g(\boldsymbol{u}, \boldsymbol{w}, \boldsymbol{n}) = -\mathbf{H}_g(\boldsymbol{w}, \boldsymbol{u}, -\boldsymbol{n})$, and locally Lipschitz-continuous.

Further, we define the viscous form

$$\begin{aligned} a_h(\boldsymbol{w}, \boldsymbol{\varphi}_h) = &\sum_{K\in\mathcal{T}_{ht}} \int_K \sum_{s=1}^{2} \mathbf{R}_s(\boldsymbol{w}, \nabla \boldsymbol{w}) \cdot \frac{\partial \boldsymbol{\varphi}_h}{\partial x_s} \, dx \\ &- \sum_{\Gamma\in\mathcal{F}_{ht}^I} \int_\Gamma \sum_{s=1}^{2} \langle \mathbf{R}_s(\boldsymbol{w}, \nabla \boldsymbol{w}) \rangle_\Gamma (\boldsymbol{n}_\Gamma)_s \cdot [\boldsymbol{\varphi}_h]_\Gamma \, dS \\ &- \sum_{\Gamma\in\mathcal{F}_{ht}^D} \int_\Gamma \sum_{s=1}^{2} \mathbf{R}_s(\boldsymbol{w}, \nabla \boldsymbol{w}) (\boldsymbol{n}_\Gamma)_s \cdot \boldsymbol{\varphi}_{h\Gamma}^{(L)} \, dS, \end{aligned} \tag{3.11}$$

(we use the incomplete discretization of viscous terms - the so-called IIPG version, symmetric and antisymmetric versions are described e.g. in [7]), the interior and boundary penalty terms and the right-hand side form, respectively,

$$J_h(\boldsymbol{w}, \boldsymbol{\varphi}_h) = \sum_{\Gamma\in\mathcal{F}_{ht}^I} \int_\Gamma \sigma [\boldsymbol{w}] \cdot [\boldsymbol{\varphi}_h]_\Gamma \, dS + \sum_{\Gamma\in\mathcal{F}_{ht}^D} \int_\Gamma \sigma \boldsymbol{w} \cdot \boldsymbol{\varphi}_{h\Gamma}^{(L)} \, dS, \tag{3.12}$$

$$\ell_h(\boldsymbol{w}, \boldsymbol{\varphi}_h) = \sum_{\Gamma\in\mathcal{F}_{ht}^D} \int_\Gamma \sum_{s=1}^{2} \sigma \boldsymbol{w}_B \cdot \boldsymbol{\varphi}_{h\Gamma}^{(L)} \, dS. \tag{3.13}$$

Here $\sigma|_\Gamma = C_W \mu / d(\Gamma)$ and $C_W > 0$ is a sufficiently large constant. The source form reads

$$d_h(\boldsymbol{w}, \boldsymbol{\varphi}_h) = \sum_{K \in \mathcal{T}_{ht}} \int_K (\boldsymbol{w} \cdot \boldsymbol{\varphi}_h) \operatorname{div} \boldsymbol{z} \, dx. \tag{3.14}$$

The boundary state $\boldsymbol{w}_B$ is defined on the basis of the Dirichlet boundary conditions and extrapolation:

$$\boldsymbol{w}_B = (\rho_D, \rho_D v_{D1}, \rho_D v_{D2}, c_v \rho_D \theta_\Gamma^{(L)} + \frac{1}{2} \rho_D |\boldsymbol{v}_D|^2) \quad \text{on } \Gamma_I, \tag{3.15}$$

$$\boldsymbol{w}_B = \boldsymbol{w}_\Gamma^{(L)} \quad \text{on } \Gamma_O, \tag{3.16}$$

$$\boldsymbol{w}_B = (\rho_\Gamma^{(L)}, \rho_\Gamma^{(L)} z_1, \rho_\Gamma^{(L)} z_2, c_v \rho_\Gamma^{(L)} \theta_\Gamma^{(L)} + \frac{1}{2} \rho_\Gamma^{(L)} |\boldsymbol{z}|^2) \quad \text{on } \Gamma_{W_t}. \tag{3.17}$$

The approximate solution is defined as $\boldsymbol{w}_h(t) \in \boldsymbol{S}_{ht}$ such that

$$\begin{aligned} \sum_{K \in \mathcal{T}_{ht}} \int_K \frac{D^A \boldsymbol{w}_h(t)}{Dt} \cdot \boldsymbol{\varphi}_h \, dx + b_h(\boldsymbol{w}_h(t), \boldsymbol{\varphi}_h) + a_h(\boldsymbol{w}_h(t), \boldsymbol{\varphi}_h) \\ + J_h(\boldsymbol{w}_h(t), \boldsymbol{\varphi}_h) + d_h(\boldsymbol{w}_h(t), \boldsymbol{\varphi}_h) = \ell_h(\boldsymbol{w}_h(t), \boldsymbol{\varphi}_h) \end{aligned} \tag{3.18}$$

holds for all $\boldsymbol{\varphi}_h \in \boldsymbol{S}_{ht}$, all $t \in (0, T)$ and $\boldsymbol{w}_h(0) = \boldsymbol{w}_h^0$ is an approximation of the initial state $\boldsymbol{w}^0$.

3.2.2 Time discretization

Let us construct a partition $0 = t_0 < t_1 < t_2 \ldots$ of the time interval $[0, T]$ and define the time step $\tau_k = t_{k+1} - t_k$. We use the approximations $\boldsymbol{w}_h(t_n) \approx \boldsymbol{w}_h^n \in \boldsymbol{S}_{ht_n}$, $\boldsymbol{z}(t_n) \approx \boldsymbol{z}^n$, $n = 0, 1, \ldots$ and introduce the function $\hat{\boldsymbol{w}}_h^k = \boldsymbol{w}_h^k \circ \mathcal{A}_{t_k} \circ \mathcal{A}_{t_{k+1}}^{-1}$, which is defined in the domain $\Omega_{ht_{k+1}}$. In order to approximate the ALE derivative at time t_{k+1}, we start from its definition and then use the backward difference:

$$\begin{aligned} &\frac{D^A \boldsymbol{w}_h}{Dt}(x, t_{k+1}) = \frac{\partial \tilde{\boldsymbol{w}}_h}{\partial t}(X, t_{k+1}) \\ &\approx \frac{\tilde{\boldsymbol{w}}_h^{k+1}(X) - \tilde{\boldsymbol{w}}_h^k(X)}{\tau_k} = \frac{\boldsymbol{w}_h^{k+1}(x) - \hat{\boldsymbol{w}}_h^k(x)}{\tau_k}, \qquad x = \mathcal{A}_{t_{k+1}}(X) \in \Omega_{ht_{k+1}}. \end{aligned} \tag{3.19}$$

By the symbol $(\cdot, \cdot)$ we shall denote the scalar product in $L^2(\Omega_{ht_{k+1}})$. A possible full discretization reads:

$$\text{(a)} \quad \boldsymbol{w}_h^{k+1} \in \boldsymbol{S}_{ht_{k+1}}, \tag{3.20}$$

$$\begin{aligned} \text{(b)} \quad &\left(\frac{\boldsymbol{w}_h^{k+1} - \hat{\boldsymbol{w}}_h^k}{\tau_k}, \boldsymbol{\varphi}_h \right) + b_h(\boldsymbol{w}_h^{k+1}, \boldsymbol{\varphi}_h) + a_h(\boldsymbol{w}_h^{k+1}, \boldsymbol{\varphi}_h) \\ &+ J_h(\boldsymbol{w}_h^{k+1}, \boldsymbol{\varphi}_h) + d_h\left(\boldsymbol{w}_h^{k+1}, \boldsymbol{\varphi}_h\right) = \ell_h(\boldsymbol{w}_h^{k+1}, \boldsymbol{\varphi}_h) \\ &\forall \boldsymbol{\varphi}_h \in \boldsymbol{S}_{ht_{k+1}}, \ k = 0, 1, \ldots. \end{aligned}$$

This problem for $\boldsymbol{w}_h^{k+1}$ is equivalent to a strongly nonlinear algebraic system and its solution is quite difficult.

Our goal is to develop a numerical scheme, which would be accurate and robust, with good stability properties and efficiently solvable. Therefore, we proceed similarly as in [4] and use a partial linearization of the forms b_h and a_h. This approach leads to a scheme that requires the solution of only one large sparse linear system on each time level. The procedure is done in way similar to the discretization of Euler equations in the previous chapter.

The linearization of the first term of the form b_h is based on the relations

$$\boldsymbol{g}_s(\boldsymbol{w}_h^{k+1}) = (\mathbb{A}_s(\boldsymbol{w}_h^{k+1}) - z_s^{k+1}\mathbb{I})\boldsymbol{w}_h^{k+1} \approx (\mathbb{A}_s(\hat{\boldsymbol{w}}_h^{k}) - z_s^{k+1}\mathbb{I})\boldsymbol{w}_h^{k+1},$$

where $\mathbb{A}_s(\mathbf{w})$ is the Jacobi matrix of $\boldsymbol{f}_s(\mathbf{w})$, cf. [6]. The second term of b_h is linearized with the aid of the Vijayasundaram numerical flux (cf. [16]) defined in the following way. Taking into account the definition of $\boldsymbol{g}_s$, we have

$$\frac{D\boldsymbol{g}_s(\boldsymbol{w})}{D\boldsymbol{w}} = \frac{D\boldsymbol{f}_s(\boldsymbol{w})}{D\boldsymbol{w}} - z_s\mathbb{I} = \mathbb{A}_s - z_s\mathbb{I}, \tag{3.21}$$

and can write

$$\mathbb{P}_g(\boldsymbol{w},\boldsymbol{n}) = \sum_{s=1}^{2} \frac{D\boldsymbol{g}_s(\boldsymbol{w})}{D\boldsymbol{w}} n_s = \sum_{s=1}^{2} \left(\mathbb{A}_s n_s - z_s n_s \mathbb{I}\right). \tag{3.22}$$

By [6], this matrix is diagonalizable. It means that there exists a nonsingular matrix $\mathbb{T} = \mathbb{T}(\boldsymbol{w},\boldsymbol{n})$ such that

$$\mathbb{P}_g = \mathbb{T}\mathbb{\Lambda}\mathbb{T}^{-1}, \quad \mathbb{\Lambda} = \mathrm{diag}(\lambda_1,\ldots,\lambda_4), \tag{3.23}$$

where $\lambda_i = \lambda_i(\boldsymbol{w},\boldsymbol{n})$ are eigenvalues of the matrix $\mathbb{P}_g$. Now we define the "positive" and "negative" parts of the matrix $\mathbb{P}_g$ by

$$\mathbb{P}_g^{\pm} = \mathbb{T}\mathbb{\Lambda}^{\pm}\mathbb{T}^{-1}, \quad \mathbb{\Lambda}^{\pm} = \mathrm{diag}(\lambda_1^{\pm},\ldots,\lambda_4^{\pm}), \tag{3.24}$$

where $\lambda^+ = \max(\lambda,0),\ \lambda^- = \min(\lambda,0)$. Using the above concepts, we introduce the modified Vijayasundaram numerical flux (cf. [16] or [6]) as

$$\boldsymbol{H}_g(\boldsymbol{w}_L,\boldsymbol{w}_R,\boldsymbol{n}) = \tilde{\mathbb{P}}_g^{+}\left(\frac{\boldsymbol{w}_L+\boldsymbol{w}_R}{2},\boldsymbol{n}\right)\boldsymbol{w}_L + \tilde{\mathbb{P}}_g^{-}\left(\frac{\boldsymbol{w}_L+\boldsymbol{w}_R}{2},\boldsymbol{n}\right)\boldsymbol{w}_R. \tag{3.25}$$

Using the above definition of the numerical flux, we introduce the approximation

$$\mathbf{H}_g(\boldsymbol{w}_{h\Gamma}^{k+1(L)},\boldsymbol{w}_{h\Gamma}^{k+1(R)},\boldsymbol{n}_\Gamma) \approx \mathbb{P}_g^{+}(\langle\hat{\boldsymbol{w}}_h^k\rangle_\Gamma,\boldsymbol{n}_\Gamma)\boldsymbol{w}_{h\Gamma}^{k+1(L)} + \mathbb{P}_g^{-}(\langle\hat{\boldsymbol{w}}_h^k\rangle_\Gamma,\boldsymbol{n}_\Gamma)\hat{\boldsymbol{w}}_{h\Gamma}^{k(R)}.$$

In this way we get the form

$$\begin{aligned}
&\hat{b}_h(\hat{\boldsymbol{w}}_h^k, \boldsymbol{w}_h^{k+1}, \boldsymbol{\varphi}_h) \qquad (3.26)\\
&= -\sum_{K\in\mathcal{T}_{ht_{k+1}}} \int_K \sum_{s=1}^{2} (\mathbb{A}_s(\hat{\boldsymbol{w}}^k(x)) - z_s^{k+1}(x))\mathbb{I})\boldsymbol{w}^{k+1}(x)) \cdot \frac{\partial \boldsymbol{\varphi}_h(x)}{\partial x_s} dx\\
&+ \sum_{\Gamma\in\mathcal{F}^I_{ht_{k+1}}} \int_\Gamma \Big(\mathbb{P}_g^+\big(\langle \hat{\boldsymbol{w}}_h^k \rangle, \boldsymbol{n}_\Gamma\big)\boldsymbol{w}_h^{k+1(L)} + \mathbb{P}_g^-\big(\langle \hat{\boldsymbol{w}}_h^k \rangle, \boldsymbol{n}_\Gamma\big)\boldsymbol{w}_h^{k+1(R)} \Big) \cdot [\boldsymbol{\varphi}_h] dS\\
&+ \sum_{\Gamma\in\mathcal{F}^B_{ht_{k+1}}} \int_\Gamma \Big(\mathbb{P}_g^+\big(\langle \hat{\boldsymbol{w}}_h^k \rangle, \boldsymbol{n}_\Gamma\big)\boldsymbol{w}_h^{k+1(L)} + \mathbb{P}_g^-\big(\langle \hat{\boldsymbol{w}}_h^k \rangle, \boldsymbol{n}_\Gamma\big)\hat{\boldsymbol{w}}_h^{k(R)} \Big) \cdot \boldsymbol{\varphi}_h dS.
\end{aligned}$$

The linearization of the form a_h is based on the fact that $\mathbf{R}_s(\boldsymbol{w}_h, \nabla \boldsymbol{w}_h)$ is linear in $\nabla \boldsymbol{w}$ and nonlinear in $\boldsymbol{w}$. We get the linearized viscous form

$$\begin{aligned}
\hat{a}_h(\hat{\boldsymbol{w}}_h^k, \boldsymbol{w}_h^{k+1}, \boldsymbol{\varphi}_h) &= \sum_{K\in\mathcal{T}_{ht_{k+1}}} \int_K \sum_{s=1}^{2} \mathbf{R}_s(\hat{\boldsymbol{w}}_h^k, \nabla \boldsymbol{w}_h^{k+1}) \cdot \frac{\partial \boldsymbol{\varphi}_h}{\partial x_s}\, dx \qquad (3.27)\\
&- \sum_{\Gamma\in\mathcal{F}^I_{ht_{k+1}}} \int_\Gamma \sum_{s=1}^{2} \big\langle \mathbf{R}_s(\hat{\boldsymbol{w}}_h^k, \nabla \boldsymbol{w}^{k+1}) \big\rangle (\boldsymbol{n}_\Gamma)_s \cdot [\boldsymbol{\varphi}_h]\, dS\\
&- \sum_{\Gamma\in\mathcal{F}^D_{ht_{k+1}}} \int_\Gamma \sum_{s=1}^{2} \mathbf{R}_s(\hat{\boldsymbol{w}}_h^k, \nabla \boldsymbol{w}_h^{k+1}) (\boldsymbol{n}_\Gamma)_s \cdot \boldsymbol{\varphi}_h\, dS.
\end{aligned}$$

Chapter 4

Fluid-Structure interaction

4.1 Description of airfoil motion

Fluid structure interaction will be discussed in this section. We derive equations describing motion of airfoil with two degrees of freedom (DOF). We assume that the airfoil is a rigid body represented by a domain Π_t. We derive equations of airfoil motion from Lagrange equations of the second kind [11]. Generalized coordinates are $h = q^1$ and $\alpha = q^2$. We assume that h is downwards positive and α is clockwise positive. As will be shown, our derivation leads to a system of two second order ordinary differential equations with unknowns h and α. These coordinates provide sufficient information about displacement and rotation of the airfoil (see Figure (4.1)). We need to consider all forces acting on the airfoil. In our case it is force caused by the flow - we call it $\vec{L}$, vertical force $\vec{M}$ and torsional force $\vec{T}$. $\vec{M}$ and $\vec{T}$ are potential forces. These forces together with viscous force $\vec{O}$ (in case of viscous flow) form total force $\vec{F} = \vec{L} + \vec{M} + \vec{T} + \vec{O}$. For the sake of simplicity gravitational force is not included.

We can write Lagrange equations of the second kind in the form

$$Q_j - \frac{d}{dt}\frac{\partial T}{\partial \dot{q}^j} + \frac{\partial T}{\partial q^j} = 0, \quad j = 1, 2. \tag{4.1}$$

T is the kinetic energy of the airfoil and Q_j is j-th component of the generalized total force corresponding to j-th generalized coordinate. $\vec{Q}$ is projection of $\vec{F}$ from Cartesian space coordinates to the generalized coordinates space h and α. We can write

$$Q_j = \sum_{i=1}^{2} F_i \frac{\partial x^i}{\partial q^i}. \tag{4.2}$$

We need one more Cartesian coordinate system x_1', x_2' coupled with the airfoil. The origin of coordinates of this system is in an elastic axis EA (4.1). We further denote x_{01}, x_{02} coordinates of the elastic axis in equilibrium position.

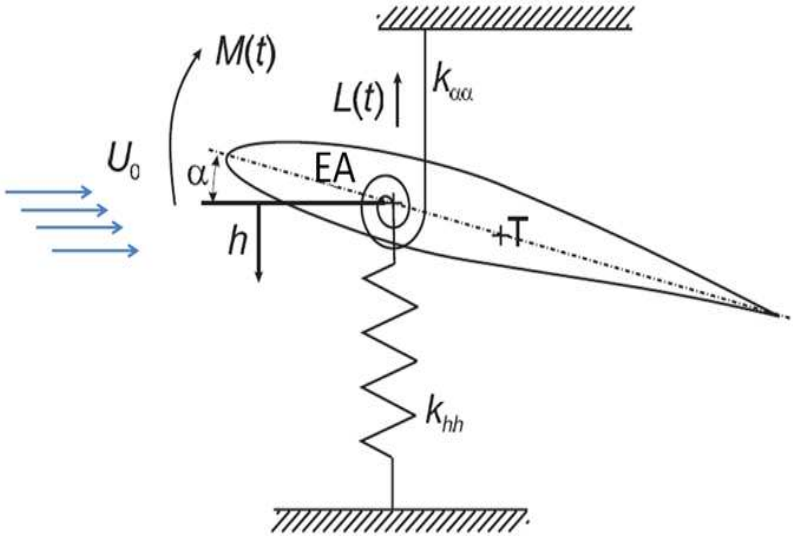

Figure 4.1: The motion of airfoil with two degrees of freedom

Moreover, we assume that axis x_1' passes through the center of gravity of airfoil as well.

We will investigate relations among the coordinate systems in the next paragraph. Arbitrary but fixed point $\boldsymbol{x}$ on airfoil has the coordinates $[x_1, x_2]$ in the referential system and coordinates $[x_1', x_2']$ in the airfoil system. The airfoil also has generalized coordinates $[h, \alpha]$. We can transform the coordinates using the relations

$$\begin{aligned} x_1 &= x_1' cos(\alpha) - x_2' sin(\alpha) + x_{01}, \\ x_2 &= x_1' sin(\alpha) + x_2' cos(\alpha) + h + x_{02}. \end{aligned} \tag{4.3}$$

Time differentiation of referential coordinates of the point $\boldsymbol{x}$ gives us

$$\begin{aligned} \dot{x}_1 &= (-x_1' sin(\alpha) - x_2' cos(\alpha))\dot{\alpha}, \\ \dot{x}_2 &= (x_1' cos(\alpha) - x_2' sin(\alpha)\dot{\alpha} + \dot{h}. \end{aligned} \tag{4.4}$$

We do not differentiate coordinates x_1', x_2', because $\boldsymbol{x}$ is fixed in this system. The total velocity $v_{\boldsymbol{x}}$ of the point $\boldsymbol{x}$ in the referential system is

$$v_{\boldsymbol{x}'}^2 = (x_1'^2 + x_2'^2)\dot{\alpha}^2 + \dot{h}^2 + 2(x_1' cos(\alpha) - x_2' sin(\alpha))\dot{h}\dot{\alpha}. \tag{4.5}$$

We shall examine all components of equation (4.1), kinetic energy T and forces $\vec{L}$, $\vec{M}$, $\vec{T}$, $\vec{O}$.

We can write the kinetic energy of airfoil as $T = \frac{1}{2}\int_{\Pi_t} \rho(\boldsymbol{x}')v_{\boldsymbol{x}'}^2$. This gives

(with our expression of velocity)

$$\begin{aligned} T &= \frac{1}{2}\dot{h}^2 \int_{\Pi_t} \rho(\boldsymbol{x}')d\boldsymbol{x}' + \frac{1}{2}\dot{\alpha}^2 \int_{\Pi_t} \rho(\boldsymbol{x}')(x_1'^2 + x_2'^2)d\boldsymbol{x}' \\ &+ \dot{h}\dot{\alpha}cos(\alpha) \int_{\Pi_t} \rho(\boldsymbol{x}')x_1' d\boldsymbol{x}' + \dot{h}\dot{\alpha}sin(\alpha) \int_{\Pi_t} \rho(\boldsymbol{x}')x_2' d\boldsymbol{x}' \\ &= \frac{1}{2}m\dot{h}^2 + \dot{h}\dot{\alpha}cos(\alpha)S_{\alpha x_1} + \dot{h}\dot{\alpha}sin(\alpha)S_{\alpha x_2} + \frac{1}{2}I_\alpha\dot{\alpha}^2, \end{aligned} \tag{4.6}$$

where:

$$\begin{aligned} I_\alpha &= \int_{\Pi_t} \rho(\boldsymbol{x}')(x_1'^2 + x_2'^2)d\boldsymbol{x}', \\ m &= \int_{\Pi_t} \rho(\boldsymbol{x}')d\boldsymbol{x}', \\ S_{\alpha x_1} &= \int_{\Pi_t} \rho(\boldsymbol{x}')x_1' d\boldsymbol{x}', \\ S_{\alpha x_2} &= \int_{\Pi_t} \rho(\boldsymbol{x}')x_2' d\boldsymbol{x}'. \end{aligned} \tag{4.7}$$

I_α is the *inertia moment* around the elastic axis EA, m is the *mass* of the airfoil. We can express $S_{\alpha x_1}$ and $S_{\alpha x_2}$ using formula of center of mass, it means

$$\begin{aligned} S_{\alpha x_1} &= \int_{\Pi_t} \rho(\boldsymbol{x}')x_1' d\boldsymbol{x}' = x_1'^T m = x_{CG}m = S_\alpha, \\ S_{\alpha x_2} &= \int_{\Pi_t} \rho(\boldsymbol{x}')x_2' d\boldsymbol{x}' = x_2'^T m = 0, \end{aligned} \tag{4.8}$$

where $x_1'^T$, $x_2'^T$ are coordinates of the center of mass of the airfoil. S_α is called *static moment around the elastic axis*, x_{CG} is the distance between elastic axis and center of mass.

Quantities in (4.7) are constant because we integrate in coordinate system coupled with airfoil and domain Π_t is time independent in this system.

We assume that vertical force $\vec{M}$ is linear with respect to h and independent of α. Using this we can write this force as

$$\vec{M}_{gen.coor.} = [M_h, M_\alpha] = -[k_{hh}h, 0], \tag{4.9}$$

where k_{hh} is model parameter called *vertical stiffness*. Potential energy corresponding to $\vec{M}$ has the form

$$V_M = \frac{1}{2}k_{hh}h^2. \tag{4.10}$$

It means

$$\vec{M}_{gen.coor.} = [M_h, M_\alpha] = -[\frac{\partial V_M}{\partial h}, \frac{\partial V_M}{\partial \alpha}]. \tag{4.11}$$

Torsional force can be modeled in a similar manner. This force is again "h-independent" and linear in α. The force is

$$\vec{N}_{gen.coor.} = [N_h, N_\alpha] = -[0, k_{\alpha\alpha}\alpha] \tag{4.12}$$

and the potential energy is

$$V_N = \frac{1}{2} k_{\alpha\alpha}\alpha^2. \tag{4.13}$$

$k_{\alpha\alpha}$ is model parameter called *torsional stiffness*.

Viscous damping forces depend on the velocity of the airfoil in fluid. For the sake of simplicity we assume these forces to be linear in generalized coordinates

$$\vec{O}_{gen.coor.} = [D_{hh}\dot{h} + D_{h\alpha}\dot{\alpha}, D_{\alpha h}\dot{h} + D_{\alpha\alpha}\dot{\alpha}]. \tag{4.14}$$

Model parameters D_{hh}, $D_{h\alpha}$, $D_{\alpha h}$ and $D_{\alpha\alpha}$ are called *viscous damping coefficients*.

4.1.1 Force caused by fluid flow

We will deal with force $\vec{L}$ in this section. This force acts at each point on the airfoil face and is generally different at each point of this face. We can write this force in the form

$$\vec{L} = \int_{\partial\Pi_t} \vec{l}(\boldsymbol{x}) ds, \tag{4.15}$$

where $\vec{l}$ is the force density and s is the airfoil parametrization.

We want to transform $\vec{L}$ to the generalized coordinates, but we cannot use the transformation (4.2) because this transformation is different in each point on the airfoil. We will transform $\vec{l}$ in every point of the airfoil and than integrate it over the airfoil surface.

We will denote the vector $\vec{l}(\boldsymbol{x})$ transformed to the generalized coordinates q^1, q^2 as $\vec{l}(\boldsymbol{x})_{gen.coor.}$. According to (4.2) we know

$$\vec{l_j}(\boldsymbol{x})_{gen.coor.} = \sum_{i=1}^{2} \vec{l}(\boldsymbol{x}) \frac{\partial x_i}{\partial q^j}, \quad j = 1, 2. \tag{4.16}$$

Using equations (4.3), we have

$$\frac{\partial x_1}{\partial h} = 0, \ \frac{\partial x_1}{\partial \alpha} = h - x_2 + x_{02}, \ \frac{\partial x_2}{\partial h} = 1, \ \frac{\partial x_2}{\partial \alpha} = x_1 - x_{01}. \tag{4.17}$$

Therefore

$$\vec{l_1}(\boldsymbol{x})_{gen.coor.} = l_2(\boldsymbol{x}), \tag{4.18}$$

$$\vec{l_2}(\boldsymbol{x})_{gen.coor.} = l_1(\boldsymbol{x})(h - x_2 + x_{02}) + l_2(\boldsymbol{x})(x_1 - x_{01}). \tag{4.19}$$

We can now express force $\vec{L}$ in generalized coordinates in form

$$L_{1\,gen.coor.} = \int_{\boldsymbol{x}\in\partial\Pi_t} l_2(\boldsymbol{x})ds = L_2, \tag{4.20}$$

$$L_{2\,gen.coor.} = \int_{\boldsymbol{x}\in\partial\Pi_t} (l_1(\boldsymbol{x})(h - x_2 + x_{02}) + l_2(\boldsymbol{x}_1)(x_1 - x_{01}))ds = -M, \tag{4.21}$$

where M is moment of force $\vec{L}$

The total force written in generalized coefficients has the form

$$\begin{aligned} \vec{Q} = [Q_1, Q_2] = [L_2, M] - [\frac{\partial V_M}{\partial h}, \frac{\partial V_M}{\partial \alpha}] \\ -[\frac{\partial V_N}{\partial h}, \frac{\partial V_N}{\partial \alpha}] + [D_{hh}\dot{h} + D_{h\alpha}\dot{\alpha}, D_{\alpha h}\dot{h} + D_{\alpha\alpha}\dot{\alpha}]. \end{aligned} \tag{4.22}$$

This gives (together with (4.6)) Lagrange equations in shape

$$L_{j\,gen.coor.} + O_{j\,gen.coor.} - \frac{d}{dt}\frac{\partial T}{\partial \dot{q}^j} + \frac{\partial(T - V_M - V_N)}{\partial q^j} = 0, \quad j = 1,\, 2. \tag{4.23}$$

We already know, how the first and second term in (4.23) look like. The third term is easily derived from (4.6) as

$$\begin{aligned} \frac{d}{dt}\frac{\partial T}{\partial \dot{h}} = m\ddot{h} + \ddot{\alpha}cos(\alpha)S_{\alpha x_1} - \dot{\alpha}^2 sin(\alpha)S_{\alpha x_1} + \\ \ddot{\alpha}sin(\alpha)S_{\alpha x_2} + \dot{\alpha}^2 cos(\alpha)S_{\alpha x_2}, \\ \frac{d}{dt}\frac{\partial T}{\partial \dot{\alpha}} = I_\alpha\ddot{\alpha} + \ddot{h}cos(\alpha)S_{\alpha x_1} - \dot{h}\dot{\alpha}sin(\alpha)S_{\alpha x_1} + \\ \ddot{h}sin(\alpha)S_{\alpha x_2} + \dot{h}\dot{\alpha}cos(\alpha)S_{\alpha x_2}. \end{aligned} \tag{4.24}$$

The last term is

$$\begin{aligned} \frac{\partial(T - V_M - V_N)}{\partial h} = -\, k_{hh}h, \\ \frac{\partial(T - V_M - V_N)}{\partial \alpha} = -\, \dot{h}\dot{\alpha}sin(\alpha)S_{\alpha x_1} + \dot{h}\dot{\alpha}cos(\alpha)S_{\alpha x_2}. \end{aligned} \tag{4.25}$$

Equation (4.23) can be now written in the form (we use also (4.8))

$$m\ddot{h} + D_{hh}\dot{h} + D_{h\alpha}\dot{\alpha} + S_\alpha\ddot{\alpha}cos(\alpha) + S_\alpha\dot{\alpha}^2 sin(\alpha) + k_{hh}h = -L_2, \tag{4.26}$$

$$I_\alpha\ddot{\alpha} + D_{\alpha\alpha}\dot{\alpha} + D_{\alpha h}\dot{h} + S_\alpha\ddot{h}cos(\alpha) + k_{\alpha\alpha}h = M. \tag{4.27}$$

These equations describe the airfoil motion. They can be linearized in the case of small amplitudes. Assuming that α and $\dot{\alpha}$ are small we can use approximation

$sin(\alpha) \approx \alpha$, $cos(\alpha) \approx 1$, $\dot{\alpha}\alpha \approx 0$, $\dot{\alpha}^2\alpha \approx 0$. This gives us the linearized form of the equations of airfoil motion

$$m\ddot{h} + D_{hh}\dot{h} + D_{h\alpha}\dot{\alpha} + S_\alpha\ddot{\alpha} + k_{hh}h = -L_2, \tag{4.28}$$

$$I_\alpha\ddot{\alpha} + D_{\alpha\alpha}\dot{\alpha} + D_{\alpha h}\dot{h} + S_\alpha\ddot{h} + k_{\alpha\alpha}h = M. \tag{4.29}$$

We can write these equations in the matrix form

$$\hat{\boldsymbol{M}}\ddot{\boldsymbol{d}}(t) + \hat{\boldsymbol{B}}\dot{\boldsymbol{d}}(t) + \hat{\boldsymbol{K}}\boldsymbol{d}(t) = \hat{\boldsymbol{f}}(t). \tag{4.30}$$

$\hat{\boldsymbol{M}}$ is the mass matrix, $\hat{\boldsymbol{B}}$ is the damping matrix and $\hat{\boldsymbol{K}}$ the stiffness matrix and

$$\hat{\boldsymbol{M}} = \begin{pmatrix} m & S_\alpha \\ S_\alpha & I_\alpha \end{pmatrix}, \quad \hat{\boldsymbol{B}} = \begin{pmatrix} D_{hh} & D_{h\alpha} \\ D_{\alpha h} & D_{\alpha\alpha} \end{pmatrix}, \quad \hat{\boldsymbol{K}} = \begin{pmatrix} k_{hh} & 0 \\ 0 & k_{\alpha\alpha} \end{pmatrix}, \tag{4.31}$$

$$\hat{\boldsymbol{f}} = \begin{pmatrix} -L_2(t) \\ M(t) \end{pmatrix}, \quad \boldsymbol{d} = \begin{pmatrix} h(t) \\ \alpha(t) \end{pmatrix}. \tag{4.32}$$

These equations are solved using fourth-order Runge-Kutta method.

Chapter 5

Used techniques

In this chapter we shall give an account of some techniques used in performed computations. We mention two different ways how to compute the lift force and the torsional moment. Further we describe technique used to modify the mesh with moving boundaries and we mention some other possibilities. Finally, the fluid-structure coupling procedure is described.

5.1 Computation of the lift force and the torsional moment acting on the airfoil

In order to solve the equations describing the airfoil movement, we need to evaluate the lift force and the moment on the right side of (4.28) and (4.29):

$$L = -l \int_{\Gamma_{W_t}} \sum_{s=1}^{2} \tau_{2s} n_s dS, \tag{5.1}$$

$$M = l \int_{\Gamma_{W_t}} \sum_{i,j=1}^{2} \tau_{ij} n_j r_i dS, \tag{5.2}$$

where τ_{ij} are components of the stress tensor

$$\mathcal{T} = (-p + \lambda \, div \, \boldsymbol{v})\mathbb{I} + 2\mu\mathbb{D}(\boldsymbol{v}), \tag{5.3}$$

see (1.23), $r_1 = -(x_2 - x_{02})$, $r_2 = (x_1 - x_{01})$, x_{01}, x_{02} are coordinates of the elastic axis, l is the depth of the airfoil, $\boldsymbol{n}$ is the unit normal pointing inside the airfoil and Γ_{W_t} is the boundary of airfoil at time t. M is assumed to be clockwise positive and L upwards positive. There are two ways to evaluate L and M:

1. *Direct evaluation* We compute the components of the stress tensor of the approximate solution on the element adjacent to the airfoil boundary,

extrapolate the components to the boundary and than integrate (5.1) using some quadrature rule.

2. *Weak formulation* The direct evaluation is not consistent with the weak formulation of the flow problem, because the pressure and space derivatives of the velocity from the weak solution do not have traces on $\partial\Omega$. We assume that $\rho, \boldsymbol{v}, p$ is a classical solution of the compressible Navier-Stokes equations (see Chapter 1) in the form

$$\frac{\partial \rho v_i}{\partial t} + \mathrm{div}(\rho v_i \boldsymbol{v}) = \rho f_i + \frac{\partial}{\partial x_i}(-p + \lambda \mathrm{div}\boldsymbol{v}) + \sum_{j=1}^{2} \frac{\partial}{\partial x_j}(2\mu d_{ij}(\boldsymbol{v})), \quad i = 1, 2. \tag{5.4}$$

We start with the lift force L. Let $\varphi \in \boldsymbol{S}_h$ be a function satisfying $\varphi|_{\Gamma_{W_t}} = 1$ and $\varphi = 0$ at all nodes outside the airfoil. We multiply (5.4) by φ, integrate over Ω, use Green's theorem and use properties of φ. We arrive at the relation

$$L = -\sum_{K \in \mathcal{T}_{PROF}} \int_\Gamma \left\{ \left(\frac{\partial(\rho v_i)}{\partial t} + \mathrm{div}(\rho v_i \boldsymbol{v}) - \rho f_i \right) \varphi \right. \tag{5.5}$$

$$\left. + (-p + \lambda \mathrm{div}\boldsymbol{v}) \frac{\partial \varphi}{\partial x_i} + 2\mu \sum_{j=1}^{2} d_{ij}(\boldsymbol{v}) \frac{\partial \varphi}{\partial x_j} \right\} dx, \quad i = 1, 2, \tag{5.6}$$

where $\mathcal{T}_{PROF}$ denotes the set of all elements with a face or a vertex lying on the airfoil. We use some quadrature rule to compute the integrals over K and finite difference to compute the time derivative.

We follow very similar process to compute torsional moment M. As a test function we use function $\boldsymbol{v}^{ort} = (v_1^{ort}, v_2^{ort}) = (r_1^{ort}, r_2^{ort})\varphi$, where $r_1^{ort} = -(x_2 - x_{02})$, $r_2^{ort} = x_1 - x_{02}$.

In our computations we use the first approach for simplicity. The ordinary differential equations (4.30) are solved by the fourth-order Runge-Kutta method. In order to employ this method and to compute the solution at the time steps $(t_{n+1/2})$ and (t_{n+1}) we need to compute (or guess) L and M at these time steps. We use the linear extrapolation

$$L(t_{n+1}) = 2L(t_n) - L(t_{n-1}), \tag{5.7}$$

$$M(t_{n+1}) = 2M(t_n) - M(t_{n-1}), \tag{5.8}$$

$$L(t_{n+1/2}) = L(t_n) + (L(t_n) - L(t_{n-1}))/2, \tag{5.9}$$

$$M(t_{n+1/2}) = M(t_n) + (M(t_n) - M(t_{n-1}))/2. \tag{5.10}$$

5.2 Mesh deformation - ALE mapping

Now we shall describe the construction of the ALE mapping. We use notation introduced in Section 2.2. We begin with the reference configuration Ω_{ref} and we assume that we know the rotation α and the vertical displacement h at time t. These values determine the position of the airfoil in Ω_t. In order to construct the ALE mapping $\mathcal{A}_t : \Omega_{ref} \to \Omega_t$, we consider two circles with the common center at the elastic axis of the airfoil and divide the reference domain into three subdomains. The inner subdomain $\Omega_{0_{in}}$ contains the airfoil and is bounded by the smaller circle. The outer subdomain $\Omega_{0_{out}}$ is bounded by the bigger circle and the exterior domain boundaries. The last subdomain $\Omega_{0_{mid}}$ is $\Omega_{0_{mid}} = \Omega_{ref} \backslash (\Omega_{0_{in}} \cup \Omega_{0_{out}})$. See Figure 5.1.

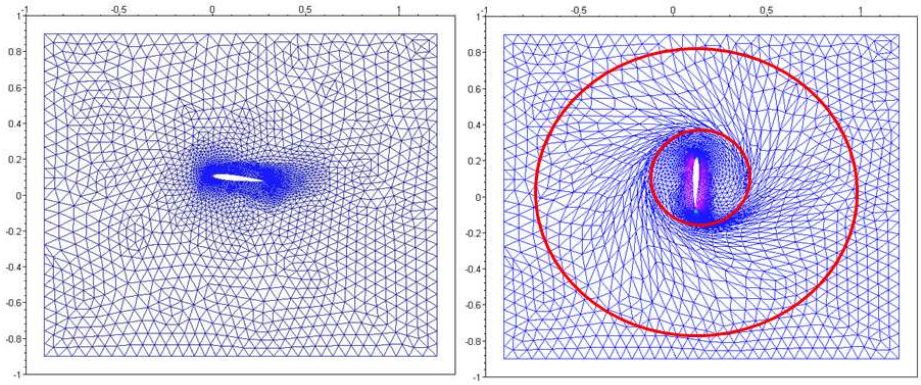

Figure 5.1: Mesh deformation, left - deformed, right - undeformed

Further, we denote the radius of the smaller circle by a and the radius of the bigger circle by b.

We prescribe the movement of the inner subdomain $\Omega_{0_{in}}$ to be the same as the airfoil movement:

$$x_1 = (X_{1\,ref} - x_{01}) \cos\alpha - (X_{2\,ref} - x_{02}) \sin\alpha + X_{1\,ref}, \tag{5.11}$$

$$x_2 = (X_{1\,ref} - x_{01}) \sin\alpha - (X_{2\,ref} + x_{02}) \cos\alpha + X_{2\,ref} + h, \tag{5.12}$$

where x_{01} and x_{02} are the coordinates of the elastic axis and $\boldsymbol{X} \in \Omega_{0_{in}}$. We denote this mapping by F_{in} having

$$\boldsymbol{x} = \mathcal{A}_t(\boldsymbol{X}) = F_{in}(\boldsymbol{X}), \quad \boldsymbol{X} \in \Omega_{0_{in}}. \tag{5.13}$$

We assume the subdomain $\Omega_{0_{out}}$ to be "frozen" in time. It means that

$$\boldsymbol{x} = \mathcal{A}_t(\boldsymbol{X}) = F_{out}(\boldsymbol{X}) = \boldsymbol{X}, \quad \boldsymbol{X} \in \Omega_{0_{out}}. \tag{5.14}$$

In the annulus $\Omega_{0_{mid}}$ the ALE mapping is defined by

$$\boldsymbol{x} = \mathcal{A}_t(\boldsymbol{X}) = \lambda F_{out}(\boldsymbol{X}) + (1 - \lambda) F_{in}(\boldsymbol{X}), \quad \boldsymbol{X} \in \Omega_{0_{mid}}, \tag{5.15}$$

where $\lambda \in [0,1]$ and λ depends only on $\boldsymbol{X}$. We choose λ in the following way:

$$\lambda = (\cos(\pi\Phi) + 1)/2, \tag{5.16}$$

where

$$\Phi = \begin{cases} 0, & |\boldsymbol{X} - \boldsymbol{x}_{EA}| > b, \\ \frac{|\boldsymbol{X}-\boldsymbol{x}_{EA}|-a}{b-a}, & a < |\boldsymbol{X} - \boldsymbol{x}_{EA}| < b, \\ 1, & |\boldsymbol{X} - \boldsymbol{x}_{EA}| < a, \end{cases}$$

$\boldsymbol{x}_{EA} = (x_{01}, x_{02})$ are the coordinates of the elastic axis.

The knowledge of the ALE mapping at time instants t_{n-1}, t_n and $t_n + 1$ allows us to approximate the domain velocity with the aid of the second-order backward difference formula

$$\boldsymbol{z}^{n+1}(\boldsymbol{x}) = \frac{3\boldsymbol{x} - 4\boldsymbol{A}_{t_n}(\boldsymbol{A}^{-1}_{t_{n+1}}(\boldsymbol{x})) + \boldsymbol{A}_{t_{n-1}}(\boldsymbol{A}^{-1}_{t_{n+1}}(\boldsymbol{x}))}{2\tau}. \tag{5.17}$$

The realization of this method is very simple, fast and allows sufficiently large deformations without mesh degeneration. This method is not applicable to movement of an airfoil with three degrees of freedom, where the third degree is torsional movement of flap. Then we have to choose some other method, as e.g. the spring analogy described in [10] or the linear elasticity equations described in [12].

5.3 FSI coupling

In this section we describe the fluid-structure interaction procedure used in this work. We have to initialize the ALE mapping before the iteration process begins. Following the previous section we have to determine radius for both the small and the big circle and then compute λ from (5.16) for all vertices of triangulation. Having this we can start the iterative procedure

1. We start at a certain time $\delta_t < 0$ by the solution of the flow, keeping the airfoil in a fixed position given by the prescribed initial displacement h_0 and the angle of attack α_0.

2. We assume that the approximate solution of the Navier-Stokes or the Euler equations on time level t_n is known. We compute the force $L(t_n)$ and the torsional moment $M(t_n)$ using Section 5.1.

3. We use the linear extrapolation (5.7) - (5.10).

4. We compute the vertical displacement h and the angle α at time t_{n+1} as a solution of equations (4.30).

5. We change the position of airfoil according to the displacement and the angle at time t_{n+1}, then determine the ALE mapping and compute the domain velocity (5.17).

6. We compute approximate solution on time level t_{n+1}.

7. We set n:=n+1 and go to 2).

Chapter 6

Results

In this chapter we shall present results obtained by the method developed in the previous chapters. We compute both inviscid and viscous flow around an airfoil NACA0012 with two degrees of freedom. At first we show results with prescribed airfoil motion. In the last section we present results of fluid-structure interaction. We compare our DGFEM compressible results with FEM incompressible results in [14].

In all performed computations we use a mesh created by the anisotropic mesh generator [3] consisting of 1665 triangle elements with 886 vertices, see Figure 6.1. We use and modify DGFEM code written by Václav Kučera in C language [7]. Quadratic (i.e. P^2) elements are used. The computations were performed on the computer Turion64 X2 with RAM 1 GB. The CPU time increases with increasing inlet velocity and is longer for the viscous code than for the inviscid one. The time step used in our computations was 10^{-5} for first few hundred iterations and 10^{-4} for the rest.

6.1 Prescribed vibrations

First we are concerned with the numerical simulations of the viscous flow around the NACA0012 profile, where its vibrations around the elastic axis with rotation $\alpha = 10(1 + \sin(2\pi f t))$ are prescribed. Here $f = 30$ Hz, vertical displacement is zero. The elastic axis is located at 1/4 of the airfoil length closer to the leading edge on the airfoil chord. The Reynolds number is 5000 and the far-field Mach number is 0.01. In Figure 6.2 we present flow patterns, which were computed for several time instants and angles of attack. We compare the streamlines with incompressible FEM results presented in [14]. We can see relatively good agreement. The quality of results could be still improved by the use of adaptive mesh refinement.

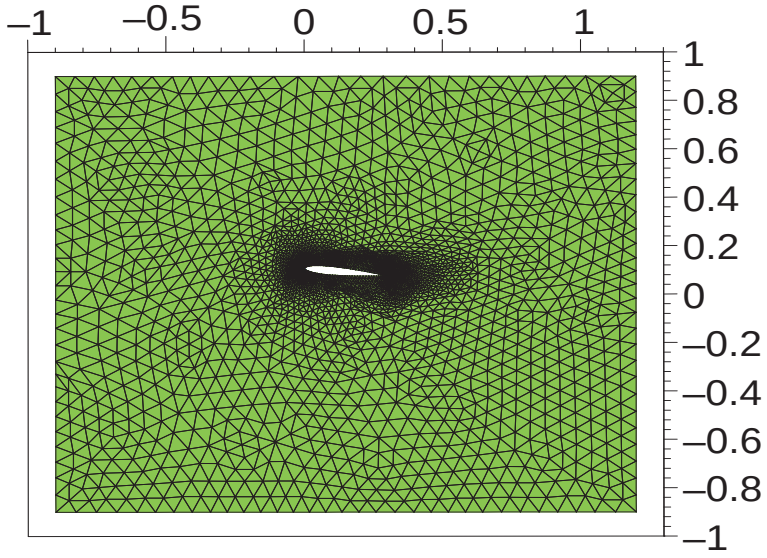

Figure 6.1: Computational mesh.

6.2 Fluid-structure interaction

Now we shall present the results of the simulation of the coupled fluid-structure interaction problem. The following quantities, used in [14], are considered: $m = 0.086622\ kg$, $S_\alpha = -0.000779673\ kg\,m$, $I_\alpha = 0.000487291\ kg\,m^2$, $k_{hh} = 105.109\ N/m$, $k_{\alpha\alpha} = 3.695582\ Nm/rad$, $l = 0.05\ m$, $c = 0.3\ m$, $\rho = 1.225\ kg/m^3$, $\nu = 1.5 \cdot 10^{-5}\ m/s^2$. The damping coefficients are considered in the form $D_{HH} = D_{\alpha\alpha} = D_{H\alpha} = D_{\alpha H} = 0$. The position of the elastic axis of the airfoil measured along the chord from the leading edge is $x_{01} = 0.4c = 0.12\,m$. Boundary conditions are $\dot{\alpha} = 0,\ \dot{h} = 0,\ \alpha = 1.407\ (6°)$ and $h = -20\ mm$.

We present subsonic inviscid and viscous results and transonic inviscid and viscous results.

6.2.1 Subsonic flow

We compare the results to the incompressible viscous results obtained by Sváček by FEM. To simulate the incompressible flow we use far-field Mach number $M = 0.014$. The computations were performed for inlet velocities $5\,m/s$, $25\,m/s$ and $40\,m/s$. In the inviscid as well as the viscous computations we use shock capturing technique presented in Section 2.1.4 with $\nu_1 = \nu_2 = 0.1$, see (2.63) and (2.64).

The differences between the inviscid and viscous results are small for $5\,m/s$, we can observe that the vibration of the airfoil in viscous flow is "slower" then the in the inviscid case. With increasing inlet velocity we can see more differences. The viscous part of the lift force and the torsional moment were much smaller than the pressure part. The vibrations are damped for $5\,m/s$ and $25\,m/s$.

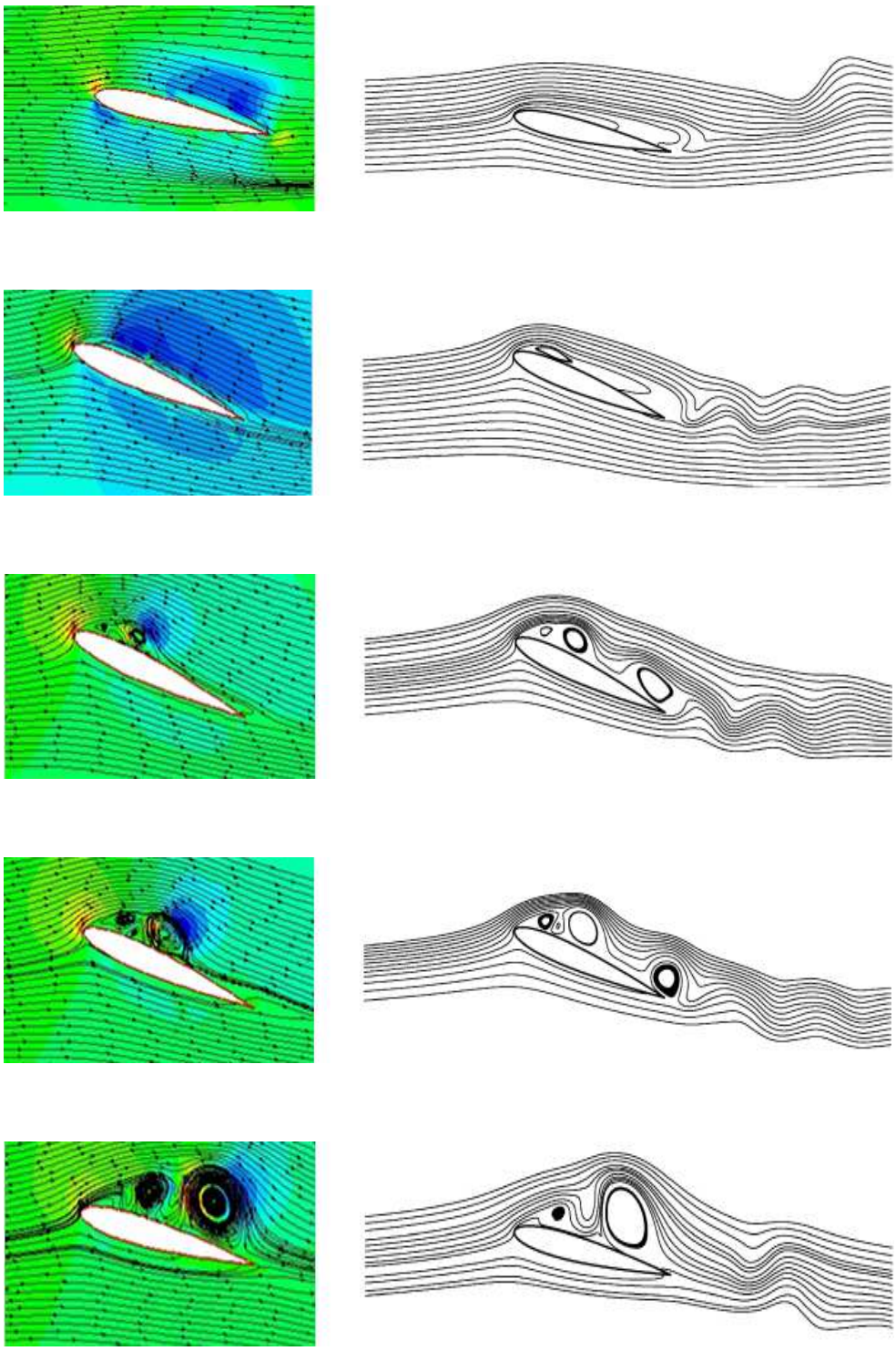

Figure 6.2: Streamlines of the flow around a moving NACA0012 airfoil for different angles of attack, left DGFEM, right FEM.

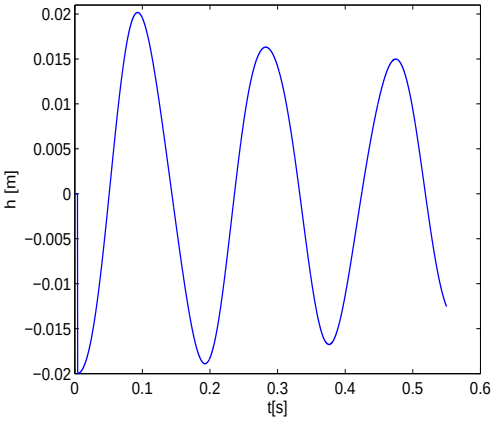

Figure 6.3: $5\,m/s$, inviscid, h.

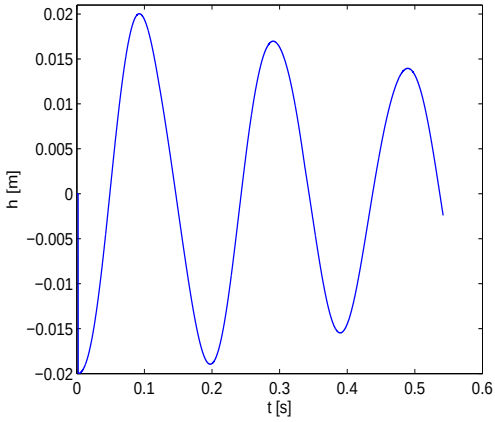

Figure 6.4: $5\,m/s$, viscous, h.

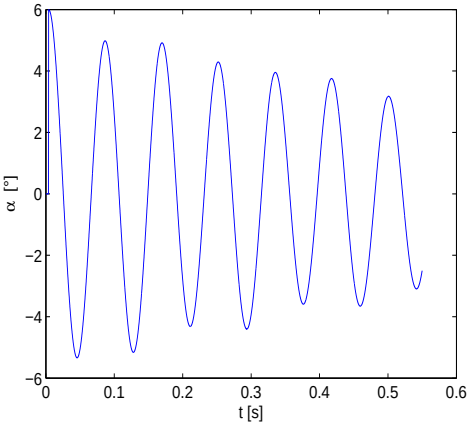

Figure 6.5: $5\,m/s$, inviscid, α.

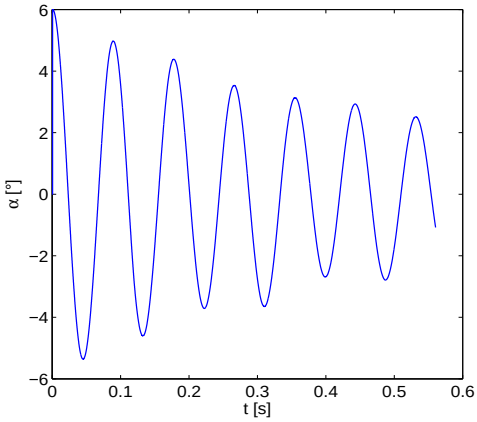

Figure 6.6: $5\,m/s$, viscous, α.

The vibration of the airfoil becomes unstable for $40\,m/s$. Mach isolines at time $t \approx 0.4\,s$ are on Figure 6.18. We can observe vortex shedding.

In Figures (6.15) – (6.17) we show the results from the viscous incompressible FEM results for $5\,m/s$, $25\,m/s$ and $40\,m/s$. We can observe very good agreement with our viscous DGFEM results in Figures (6.4), (6.6), (6.8), (6.10), (6.12), (6.14).

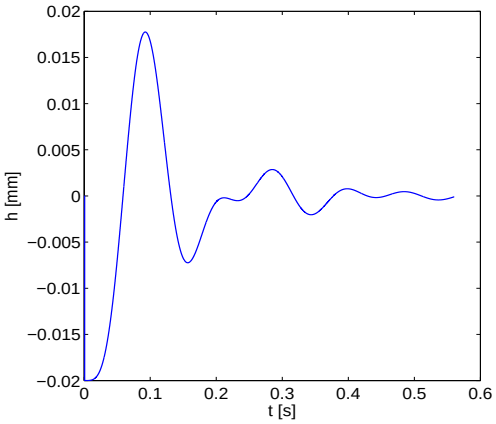

Figure 6.7: $25\,m/s$, inviscid, h.

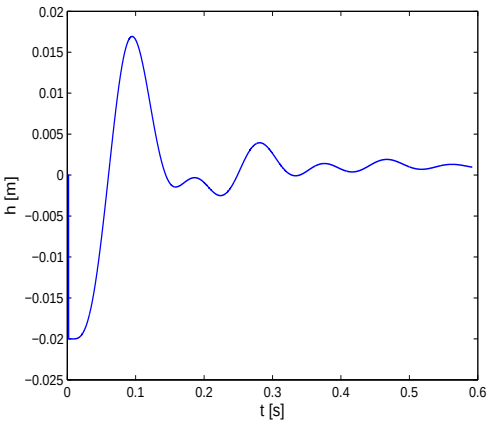

Figure 6.8: $25\,m/s$, viscous, h.

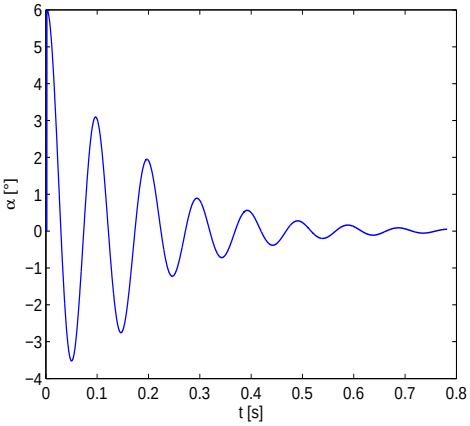

Figure 6.9: $25\,m/s$, inviscid, α.

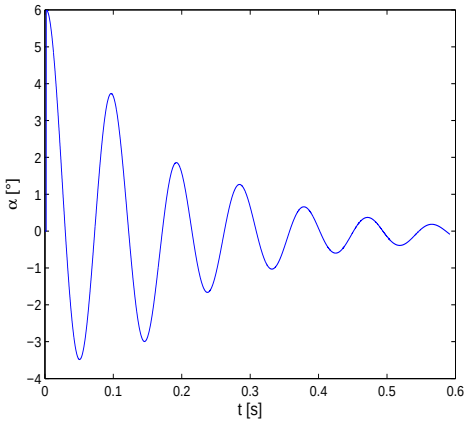

Figure 6.10: $25\,m/s$, viscous, α.

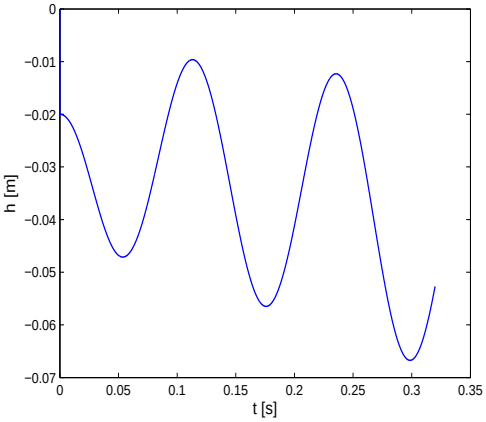

Figure 6.11: $40\,m/s$, inviscid, h.

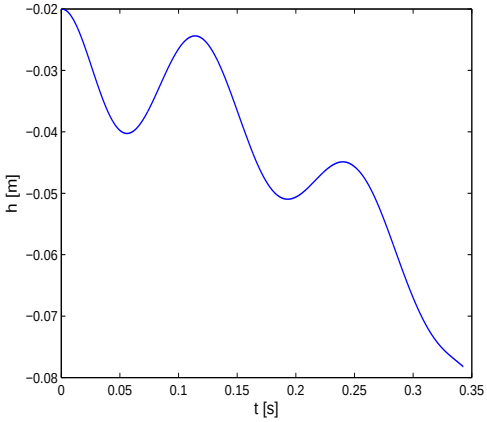

Figure 6.12: $40\,m/s$, viscous, h.

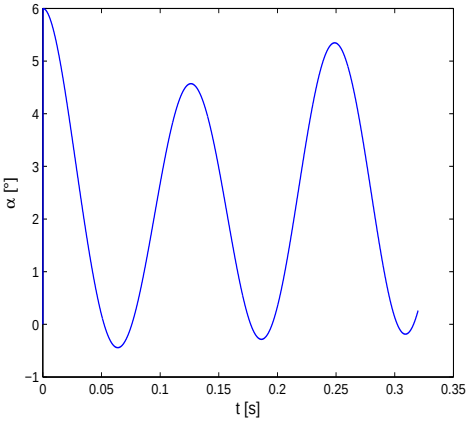

Figure 6.13: $40\,m/s$, inviscid, α.

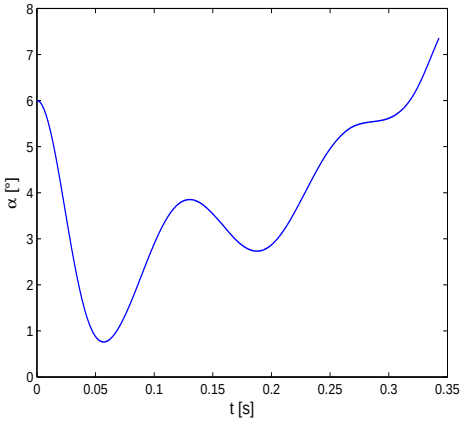

Figure 6.14: $40\,m/s$, viscous, α.

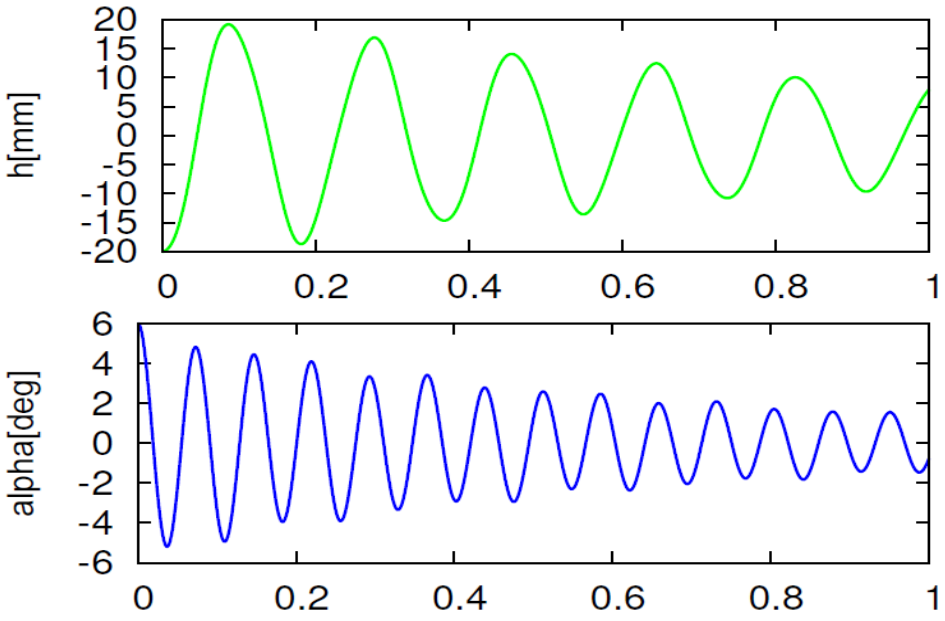

Figure 6.15: $5\,m/s$, incompressible, FEM.

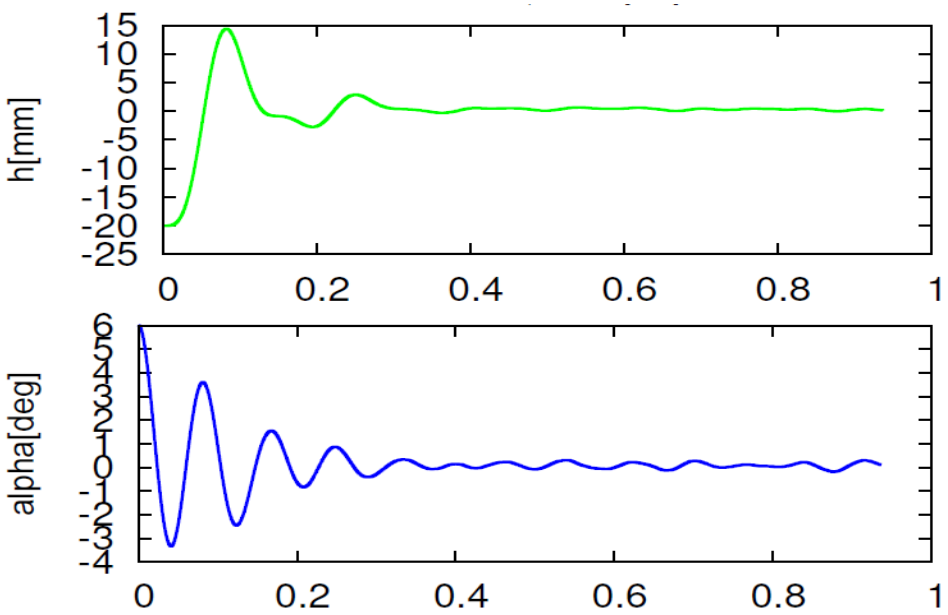

Figure 6.16: $25\,m/s$, incompressible, FEM.

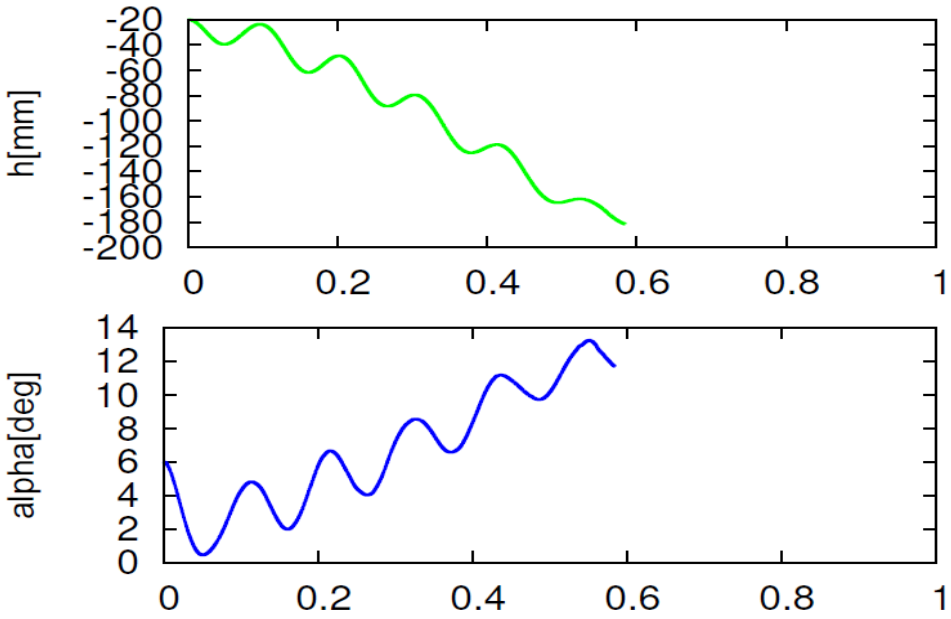

Figure 6.17: $40\,m/s$, incompressible, FEM.

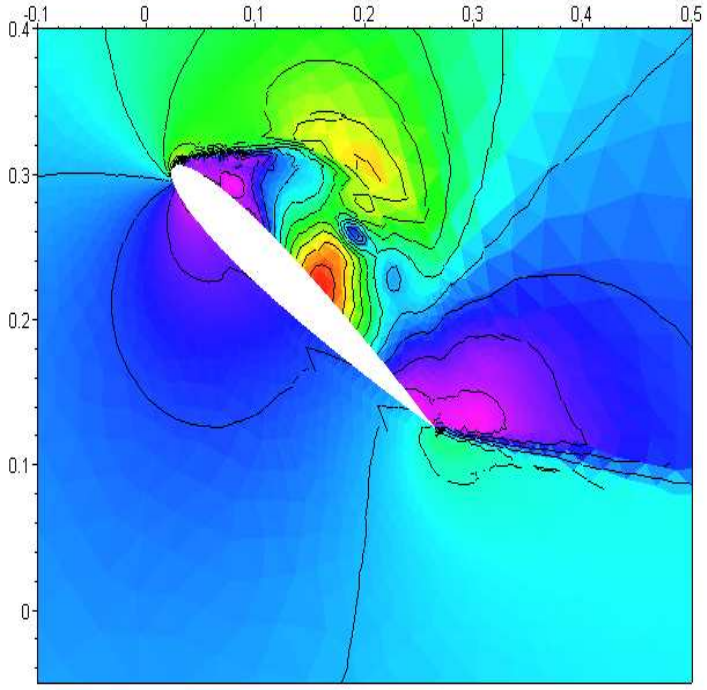

Figure 6.18: Mach isolines, unstable solution, $40\,m/s$, $t \approx 0.4\,s$.

6.2.2 Transonic flow

We performed calculations with far-field Mach number $M = 0.8$ resulting in the transonic flow. The far-field velocity was set to $25\,m/s$. If we compare Figures 6.20 and 6.19 with 6.9 and 6.7, we can see that the effect of compressibility is strong and that the solutions are quite different.

In the shock capturing technique presented in Section 2.1.4 we first used $\nu_1 = \nu_2 = 0.1$. This setting caused computation collapse for both the viscous and inviscid flow when the shock wave started to evolve. Increasing the constants to $\nu_1 = \nu_2 = 0.2$ is sufficient for the viscous computation while the inviscid computation still collapses. Further, the settings $\nu_1 = \nu_2 = 0.2$ also led to the code collapse in viscous case for far-field $M = 0.9$. Setting $\nu_1 = \nu_2 = 1$ is sufficient for the viscous and inviscid flow. Shock capturing technique proved to be necessary for transonic flow computations.

In Figures 6.21 - 6.26 the Mach number isolines obtained for inviscid flow are shown at different time instant and angles of attack. We can see the shock wave traveling as the airfoil vibrates. Figure 6.26 shows the Mach number isolines when the airfoil vibrations are damped.

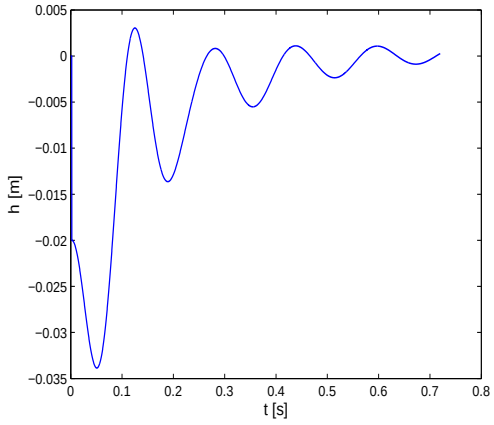

Figure 6.19: Transonic, $25\,m/s$, inviscid, h.

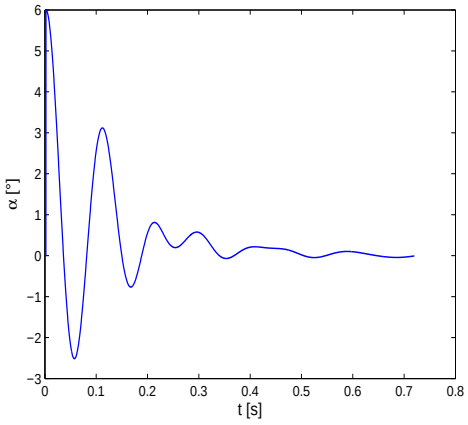

Figure 6.20: Transonic, $25\,m/s$, inviscid, α.

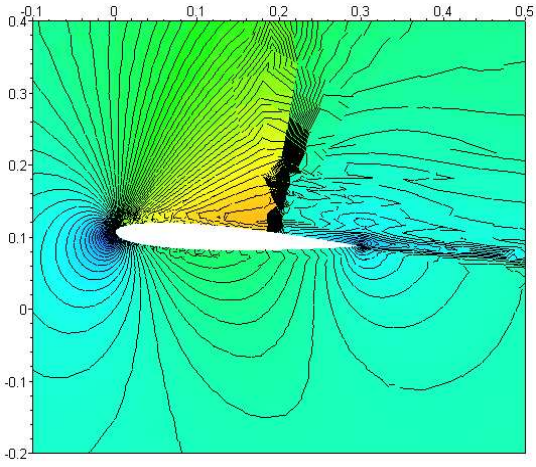

Figure 6.21: Mach isolines, far-field Mach number 0.8, $t = 0.03\,s$.

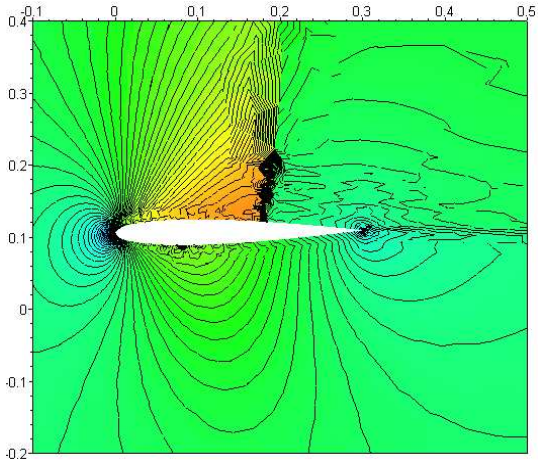

Figure 6.22: Mach isolines, far-field Mach number 0.8, $t = 0.06\,s$.

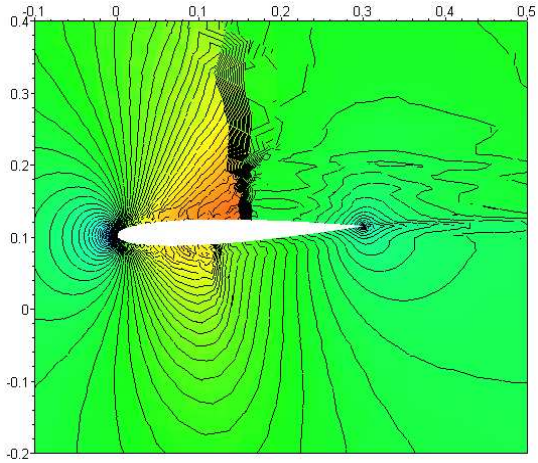

Figure 6.23: Mach isolines, far-field Mach number 0.8, $t = 0.09\,s$.

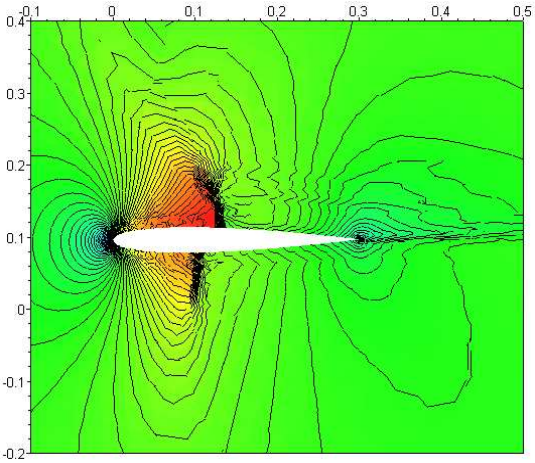

Figure 6.24: Mach isolines, far-field Mach number 0.8, $t = 0.12\,s$.

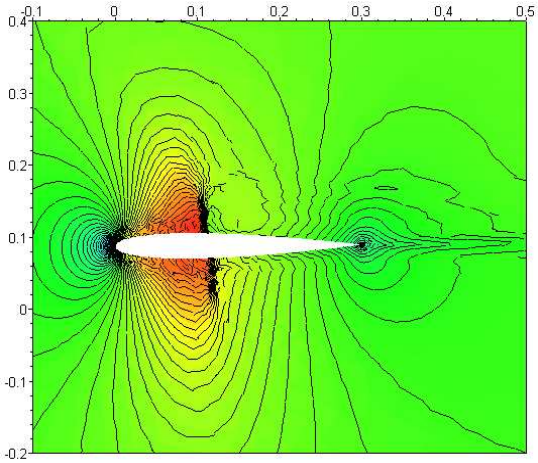

Figure 6.25: Mach isolines, far-field Mach number 0.8, $t = 0.15\,s$.

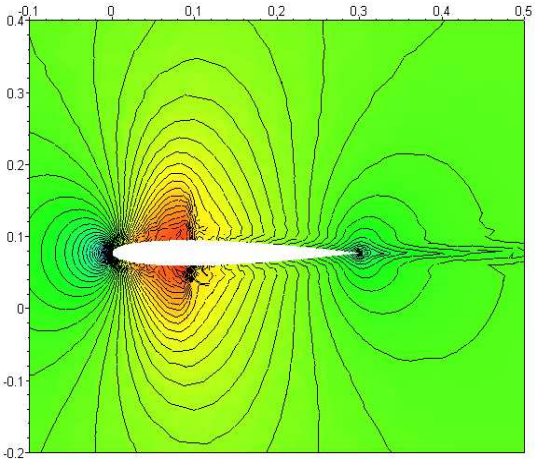

Figure 6.26: Mach isolines, far-field Mach number 0.8, $t = 0.3\,s$.

Conclusion

We have derived and formulated Euler and Navier-Stokes equations, the continuity equation and the energy equation in the first Chapter.

Next, the discretization of the Euler equations by the discontinuous Galerkin finite element method is presented. The space semidiscretization and time discretization is performed for time-independent and time-dependent computational domain. The Vijayasundaram numerical flux is used. The way how to treat the boundary conditions and shock capturing technique is presented.

In the Chapter 3 we show the space semidiscretization and the time discretization of the compressible Navier-Stokes equations in time-dependent domain based on the DGFEM.

Chapter 4 is devoted to the derivation of the equations describing the motion of airfoil with two degrees of freedom.

The fluid-structure coupling, mesh-deformation method and two approaches for computing aerodynamical forces (the lift force and the torsional moment) form the contents of Chapter 5.

In the last chapter, our results are shown. At first we present results of viscous computation for prescribed motion of the airfoil, these results are compared with existing incompressible FEM results [14]. We can see good agreement, small deviations can be consequence of the compressibility or of the mesh density.

The results, when the motion of the airfoil is influenced by fluid flow surrounding the airfoil were computed for different far-field velocities. The motion was dumped for lower far-field velocities and proved to be unstable for $40\,m/s$. The results of viscous flow with low Mach number were compared with FEM incompressible results and proved good agreement. The capability of this code to compute transonic flow was examined. The necessity to use the shock capturing technique was observed and some comments on the parameters choice were mentioned.

The presented work proved that the developed method works for both viscous and inviscid flow and is able to accurately predict the fluid-structure interaction. The future work can involve 3D computation, higher number of degrees of freedom of the airfoil, some computational acceleration (p-multigrid etc.) or the use of turbulent models.

Bibliography

[1] J. Jaffre, C. Johnson, A. Szepessy, Convergence of the discontinuous Galerkin finite elements for hyperbolic conservation laws. Math. Models Methods Appl. Sci., 5 (1995) 367–386.

[2] J. Donea, A. Huerta, J.-Ph. Ponthot, A. Rodríguez-Ferra, Arbitrary Lagrangian-Eulerian methods. Encyclopedia of Computational Mechanics, (2004).

[3] V. Dolejší, Anisotropic mesh adaptation for finite volume and finite element methods on triangular meshes, Comput. Vis. Sci. 1(3) (1998) 165–178.

[4] V. Dolejší, M. Feistauer, A semi-implicit discontinuous Galerkin finite element method for the numerical solution of inviscid compressible flow, J. Comput. Phys. 198 (2004) 727–746.

[5] V. Dolejší, M. Feistauer, C. Schwab, On some aspects of the discontinuous Galerkin finite element method for conservation laws. Math. Comput. Simul. 61 (2003) 333–346.

[6] M. Feistauer, J. Felcman, I. Straškaraba, Mathematical and Computational Methods for Compressible Flow, Clarendon Press, Oxford, (2003).

[7] V. Kučera. Higher order methods of the solution of compressible flows. Doctoral Thesis. Faculty of mathematics and physics, Charles university in Prague, (2007).

[8] L. Krivodonova, M. Berger, High-order accurate implementation of solid wall boundary conditions in curved geometries, J. Comput. Phys. 211 (2006) 492–512.

[9] M. Feistauer, J. Česenek, J. Horáček, V. Kučera, J. Prokopová, DGFEM for the numerical solution of compressible flow in time dependet domains and application to fluid-structure interaction, (2010).

[10] C. Farhat, C. Degand, B. Koobus, M. Lesoinne, Torsional springs for two-dimensional dynamic unstructured fluid meshes, Comput. Methods Appl. Mech. Engrg. 163 (1998) 231-245

[11] J. Kvasnica, Mechanika, Academia, Praha, (1988).

[12] M. Ruzicka. Numerical simulation of flow induced airfoil vibrations. Doctoral Thesis. Faculty of mathematics and physics, Charles university in Prague, (2009).

[13] T. Nomura, T.J.R. Hughes, An arbitrary Lagrangian-Eulerian finite element method for interaction of fluid and a rigid body, Comput. Methods Appl. Mech. Engrg., 95 (1992) 115-138.

[14] P. Sváček, M. Feistauer, J. Horáček, Numerical simulation of flow induced airfoil vibrations with large amplitudes. J. of Fluids and Structures, 23 (2007) 391-411.

[15] J. J. W. van der Vegt, H. van der Ven, Space-time discontinuous Galerkin finite element method with dynamic grid motion for inviscid compressible flow, J. Comput. Phys. 182 (2002) 546–585.

[16] G. Vijayasundaram, Transonic flow simulation using upstream centered scheme of Godunov type in finite elements, J. Comput. Phys. 63 (1986) 416–433.